Downloaded from orbit.dtu.dk on: Apr 19, 2024

DTU Library

Hardening evolution of geopolymers from setting to equilibrium: A review

Ranjbar, Navid; Kuenzel, Carsten; Spangenberg, Jon; Mehrali, Mehdi

Published in:
Cement and Concrete Composites

Link to article, DOI:
10.1016/j.cemconcomp.2020.103729

Publication date:
2020

Document Version
Publisher's PDF, also known as Version of record

Link back to DTU Orbit

Citation (APA):
Ranjbar, N., Kuenzel, C., Spangenberg, J., & Mehrali, M. (2020). Hardening evolution of geopolymers from setting to equilibrium: A review. *Cement and Concrete Composites*, *114*, Article 103729. https://doi.org/10.1016/j.cemconcomp.2020.103729

General rights
Copyright and moral rights for the publications made accessible in the public portal are retained by the authors and/or other copyright owners and it is a condition of accessing publications that users recognise and abide by the legal requirements associated with these rights.

- Users may download and print one copy of any publication from the public portal for the purpose of private study or research.
- You may not further distribute the material or use it for any profit-making activity or commercial gain
- You may freely distribute the URL identifying the publication in the public portal

If you believe that this document breaches copyright please contact us providing details, and we will remove access to the work immediately and investigate your claim.

Cement and Concrete Composites 114 (2020) 103729

Contents lists available at ScienceDirect

Cement and Concrete Composites

journal homepage: http://www.elsevier.com/locate/cemconcomp

Hardening evolution of geopolymers from setting to equilibrium: A review

Navid Ranjbar [a,b,c,*], Carsten Kuenzel [d,**], Jon Spangenberg [a], Mehdi Mehrali [a]

[a] Department of Mechanical Engineering, Technical University of Denmark, 2800, Kgs Lyngby, Denmark
[b] Department of Health Technology, Technical University of Denmark, 280, Kgs Lyngby, Denmark
[c] Department of Civil, Environmental and Geomatic Engineering, University College London, London, WC1E 6BT, UK
[d] Department of Civil and Environmental Engineering, Imperial College London, UK

ARTICLE INFO

Keywords:
Geopolymer
Setting time
Acceleration
Retardation
Compressive strength

ABSTRACT

In recent years, environmentally sustainable geopolymers have been widely investigated to obtain comparable mechanical properties with Portland cement, and they are now close to being in a position where they can substitute parts of the cement production utilized in construction. However, in order for geopolymers to reach their full potential, it is crucial to understand the influence of various parameters (e.g., particle size, treatment of precursor, chemical composition) on the hardening evolution at earlier ages of the pastes and the resulting final mechanical strength of the set system. Hence, this paper reviews known factors that influence the setting time of fresh geopolymers and discusses the underlying chemical- and physical-mechanisms of each parameter. Next to this, the interconnection between the setting time and mechanical strength is discussed. This will provide a platform for researchers and engineers to understand the hardening evolution of geopolymers in a broader range.

1. Introduction

In several applications, not only is the final mechanical strength important but also the setting time of the concrete is crucial independent of which binder is used, cement or geopolymers. Some applications such as precast fabrication, repair, rigid pavement rehabilitation/construction require concretes with fast setting, while others like transportation of ready-mix concrete over long distances demand concretes with the retarded setting. This can be even more complicated in some applications such as oil well operation and 3D printing, in which a sequence of retardation and acceleration in setting mechanism is often favorable. To explain this more, in oil well operations [1,2], if the viscosity of the slurry exceeds a few Pa.s, it becomes difficult to pump efficiently. Hence, it must remain in a fluid state for several hours, while it is pumped into place. However, to reduce valuable rig time, the slurry has to set shortly after being placed in the position [3]. Likewise, in 3D printing, the concrete should not set before being extruded in order to avoid blockage of the printing system, while it needs to set on time after deposition to carry the accumulated weight of the subsequent layers [4–6]. A similar concern is challenging in other applications that are based on pumping systems such as shotcrete technologies [7], or in pneumatic placement [8–10], slip forming [11], extrusion through a stationary die [12–14] where the binder has to gain strength enough to keep its shape without having external confinements.

For all the above-mentioned applications, ordinary Portland cement (OPC) based concretes have been the first choices [15,16]. This is not only due to availability but also because of a deep understanding of the material. However, due to increasing demand of materials with a reduced carbon footprint and low energy consumption [17,18], a burgeoning interest has been observed from academia and industry to develop, characterize, and implement novel sustainable construction materials, which are prerequisites for modern infrastructure with new standards [19–21]. One of these new proposed materials is geopolymer, a synthetic alkali aluminosilicate material produced by the reaction of aluminosilicate sources with highly concentrated aqueous alkali hydroxide or silicate solutions [22,23]. Depending on the mix design and processing conditions, geopolymers can exhibit different properties such as high early-compressive strength, acid resistance, and fire resistance [23–25]. These properties enable the binder to be used in applications such as in situ and precast construction, refractories and high-temperature applications, soil stabilization, pavement systems, and 3D printing.

Over the last years, the research focus has been on the feasibility of using this "green" binder instead or as a supplement to conventional

* Corresponding author. Department of Mechanical Engineering, Technical University of Denmark, 2800, Kgs Lyngby, Denmark.
** Corresponding author.
E-mail addresses: naran@mek.dtu.dk (N. Ranjbar), carsten.kuenzel@gmx.de (C. Kuenzel).

https://doi.org/10.1016/j.cemconcomp.2020.103729
Received 6 April 2020; Received in revised form 22 June 2020; Accepted 26 June 2020
Available online 26 July 2020
0958-9465/© 2020 The Authors. Published by Elsevier Ltd. This is an open access article under the CC BY-NC-ND license (http://creativecommons.org/licenses/by-nc-nd/4.0/).

cement applications [11,26,27]. This feasibility has been proven, and the chemical reactions have been understood. The next step in order to design the system according to the desired application is to understand the hardening evolution of the material to a greater extent, which in this paper is investigated by analyzing the effect of different parameters on the setting time as well as the correlation between this property and the final mechanical strength. To address this common but not well-discussed issue, the present study covers the latest state of the art in setting time and mechanical strength of geopolymers.

2. A brief on the reaction kinetics of geopolymer

Geopolymers are inorganic polymers based on tetrahedral linked aluminates and silicates that are produced through the dissolution of aluminosilicate sources using an alkali metal hydroxide and/or alkali silicate-solution [28]. The high pH of the activation solution initiates a dissolution reaction that is followed by precipitation. The timeline of these reactions cannot be divided clearly and occur almost simultaneously in the bulk of the material, however they can be split into two phases in microscale: I. dissolution–hydrolysis and II. hydrolysis–polycondensation [29,30]. During the dissolution-hydrolysis, the aluminate and silicate are dissolved from the solid precursor, and $Al(OH)_4^-$ and $SiO(OH)_3^-/SiO(OH)_2^{2-}$ are formed [31]. These anions have been classified as monomers that undergo first condensation reaction and form oligomers. The oligomers condense further by three dimensional cross-linking and aluminosilicate polymers with a typical formulation of $nM_2O{\cdot}Al_2O_3{\cdot}xSiO_2{\cdot}yH_2O$, where M is an alkali metal [32–34]. The kinetics of both reactions are mainly controlled by the chemical composition of precursors, structure, surface area, and temperature [35–37].

In theory, the whole aluminosilicate precursor could potentially be dissolved and polymerized. However, this has rarely been reported even for pure and highly reactive precursors such as metakaolin (MK), and unreacted particles observed in SEM images [38]. When impure waste products such as fly ash (FA) are used, unreacted particles are much more visible after the condensation reaction [28,38], i.e., in the case of FA, weakly-reactive crystalline phases such as mullite and quartz, which form the particle skeleton, and magnetite remain un-reacted [39]. Next to this, the complexity of the chemical reaction increases when other soluble ions such as calcium are present together with aluminates and silicates. In this case, other compositions such as calcium aluminosilicates and sodium-calcium aluminosilicates may be formed [40–42].

3. Methodology

In this section, the most common methods for quantifying the setting time (i.e., Vicat needle and rheology) are explained shortly. Furthermore, the approach used to interpret the long-term hardening of the geopolymer is described.

3.1. Vicat needle setting measurement

The most common method to determine the setting time is Vicat needle measurements, which is described in ASTM C191. This method is based on the resistance to penetration of a 50 mm needle with 1 mm diameter into a fresh paste under a mass of 300 ± 0.5 g at ambient temperature. The limitations of this method are that it depends on the resting time of the needle, doesn't provide information about the material hardening before the initial setting time, and is a discontinuous measurement [43,44]. However, despite these drawbacks, the Vicat needle is easy to operate and sufficiently reproducible to characterize the setting of geopolymers. Therefore, it has been widely used and is the most referred method in the present study.

3.2. Setting/gelation measurement using rheological measurement

Next to the Vicat needle, rheology is also an accepted technique to measure the setting of cement through the gelation time [45]. As discussed in Section 2, geopolymers go through a polycondensation reaction to build a fully three-dimensional cross-linked structure. The beginning of the polymerization is difficult to detect due to the low resolution of most existing conventional methods (e.g., Vicat needle measurement). However, the polymer builds up more intersections over time. The shortest time at which the polymer interaction congests enough that a transition from a liquid to a solid branched polymer occurs is called the gelation point [46]. This can be measured using a tangent crossover point method applied to the evolution of rheological parameters such as loss modulus and storage modulus over time [47–50].

3.3. Continuous hardening of geopolymers

After setting, the hardening of geopolymers continues to increase over time as measured by mechanical strength. In this study, the strength at quasi reaction equilibrium, point "b", is used as an index for the final compressive strength of the material, point "c", see Fig. 1. This is due to the fact that at this point, a stable structure has been formed. Previous studies have shown that this point is reached within 90 days for most of the geopolymers [51,52]. Hence, the strength obtained at this age has been used to correlate with the setting time results when it was available. Noteworthy, when the 90th-day compressive strength was not available the latest strength has been used.

4. Effects aluminosilicate sources

A wide range of aluminosilicates can be used as precursors, and their chemical composition influences the geopolymer properties. Therefore, a direct comparison of different research papers is difficult. Despite this drawback, it is still possible to identify clear trends in the influence of important parameters including, specific surface area, reactivity, chemical compositions, and alkali activators on the hardening evolution

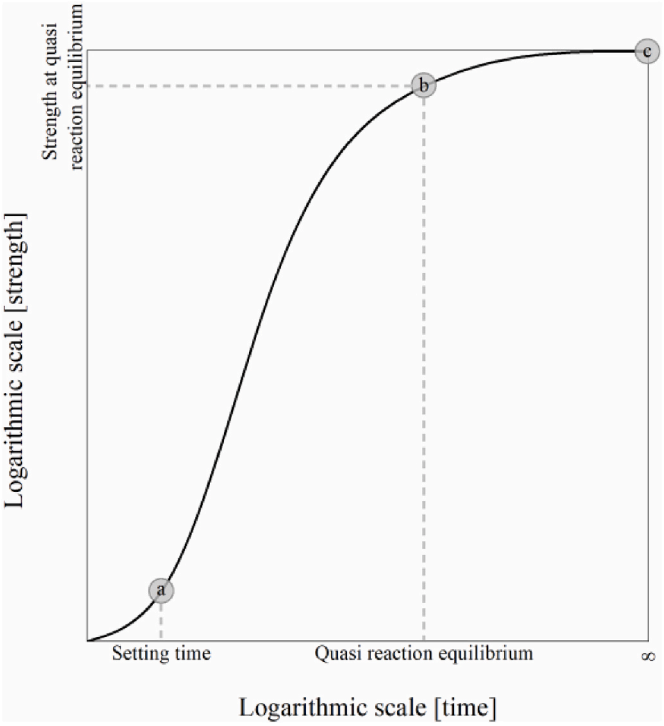

Fig. 1. Conceptual hardening evolution of geopolymers.

of geopolymers.

4.1. Particle size distribution/specific surface area

As described earlier, geopolymerization is a reaction based on the sequence of dissolution, hydrolysis, and polycondensation. The most important step for the dissolution is the interaction of the liquid and solid phases. This is affected by both the wettability of the solid source and the surface area, which can interact with the activation solution. The wettability of solid aluminosilicates is challenging to measure due to the size limitation. However, it can be assumed similar for all geopolymer precursors because they are mostly aluminosilicates. Besides, the activation solution is often either sodium hydroxide or potassium hydroxide with additional sodium silicate or potassium silicate. Therefore, only the surface area remains as a factor, and once the particle size distribution is known, a rough estimation of the surface area is possible. This estimation cannot be presented by a unique correlation, but samples with a smaller particle size distribution have an increased surface area [53–55].

To increase the surface area of a specific sample, two methods can be used: 1) sieving/separation of the solid material [56,57], and 2) grinding of the source [55,58–62]. Fig. 2 demonstrates both methods. The sieving/separation method can be further split into two: a) sieving, and b) separation by density differences, see Fig. 2b–d. These approaches have been used to investigate the effects of preprocessing of aluminosilicates on the setting time and mechanical strength of the corresponding geopolymers [55–62].

In principle when waste sources are used, the chemical composition of the separated/sieved fractions is not necessarily similar [39,63]. This is because waste sources contain a mixture of various particles, and each can have its own chemical composition or crystal structure [39]. This means that the particles obtained through sieving/separation techniques can have a different chemical composition and crystal structure [56,57]. In this case, different setting times and mechanical properties are expected. However, when a sample is milled, it can be assumed that the chemical composition and the crystal structure remain similar because the whole batch is milled, and nothing is removed or added. Only in cases of milling with high energy, a slight crystal change is expected [64]. This crystal change may result in the formation of more amorphous material, which in turn influences in setting time and compressive strength [65]. This will be discussed in detail in Section 4.2.

Fig. 3a compares the influence of particle size on both the final setting time and the compressive strength of the pastes for three different waste materials. To improve the evaluation of the results, the chemical composition, as well as the amount of amorphous material, are presented in Table 1. In general, the data show that decreasing the particle size reduces the setting time and increases mechanical properties. This influence on setting time is due to two effects: the amount of amorphous material and change in surface area. The data show that smaller particles have a higher amount of amorphous materials, which can be directly correlated with reactivity. The more amorphous material is available, the more can react. Next to this, smaller particles have a larger surface area, meaning more surface area is in contact with the activation solution, hence dissolution is “faster” and more material can react.

The increase of compressive strength with decreasing particle size was surprising because it was expected that the dissolution of solid sources continues until all reactive materials are dissolved, and therefore, leads to similar mechanical properties. This theory is based on reactivity measurements using the dissolution method that 1 g of the solid source is placed in 100 ml of the activation solution for 24 h at a curing temperature of 65 °C [66]. Due to the fact that the compressive strength is higher when smaller particles have been used, it can be implied that an aluminosilicate layer is built-up on the particle surface which reduces the dissolution of further $Al(OH)_4^-$ and $SiO_2(OH)_2^{2-}$/$SiO(OH)_3^-$, Fig. 3b. This layer protects the inner core of the particles against the chemical reaction, and consequently, the particles remain partially reacted in the system [32]. To support this theory, several solid particles have been observing in backscattered electron (BSE) imaging of geopolymer cross-section, which is proof of incomplete reaction of the reactive aluminosilicate particles. Fig. 3c and d show the morphology of FA based geopolymers and the residue after the reactivity test, respectively. Fig. 3c points out that next to the geopolymer matrix, partially reacted FA, cenospheres, and un-reactive particles can be identified.

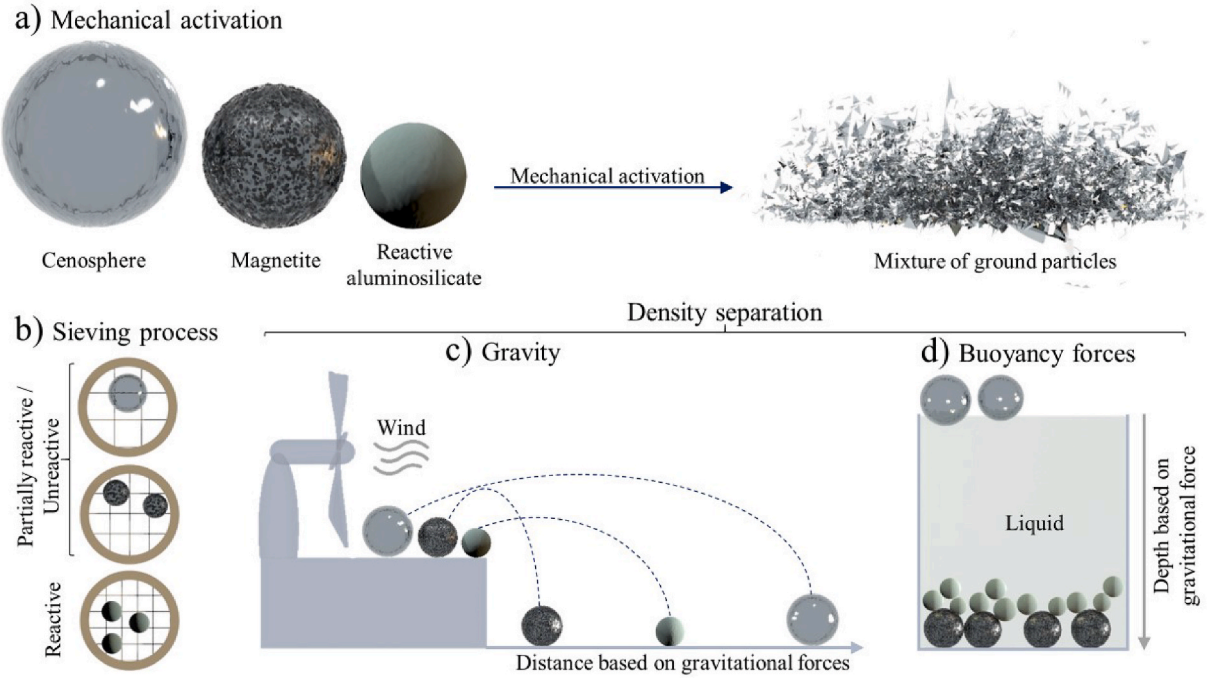

Fig. 2. Correlation between FA composition before and after a) mechanical activation; b) sieving process; c) air classification; d) wet classification. The concepts have been obtained from Refs [39, 55, 56, 65–67].

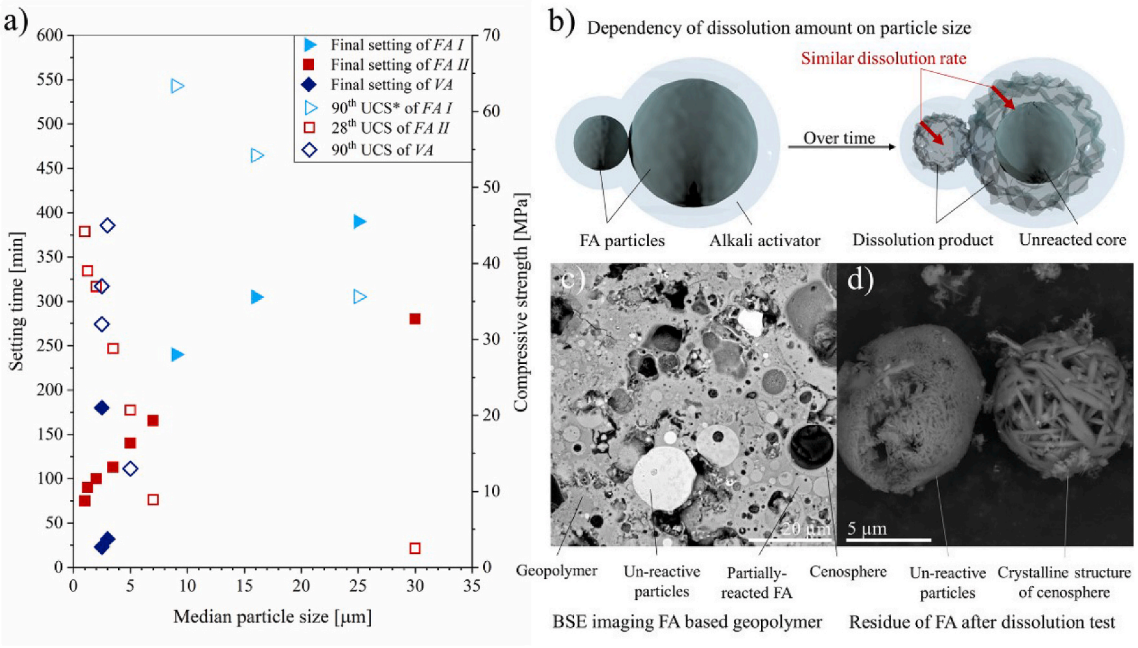

Fig. 3. a) Effect of particle size on Vicat setting time of geopolymers; b) schematic of the difference in the reaction of small and large particles; c) typical BSE image of the cross-section of FA based geopolymer; d) scanning electron microscopy image of residue in reactivity test. Note: Fig c [68] and d [66] are original images from our previous studies. Other data have been collected from Ref. [55–57,59,69].

Table 1
Chemical composition of the aluminosilicate sources used in Fig. 3.

Materials	Remarks	Median particle size [μm]	SiO_2	Al_2O_3	Fe_2O_3	CaO	MgO	Na_2O	K_2O	LOI	Amorphousness [%]
FA I [56]	One type of FA have sieved to get three classes of material	25	45.03	23.98	10.68	13.34	3.39	0.08	2.41	0.54	70–75
		16	44.35	23.37	10.31	14.46	3.30	0.05	2.72	0.97	75–85
		9	44.39	23.36	10.36	13.08	3.37	0.09	2.66	0.98	85–90
FA II [55]	One source of FA have been ground at different intervals of 0, 5, 10, 20, 45, 60, and 90 min[a]	30, 7, 5, 3.5, 2, 1.25, and 1	60.48	28.15	4.52	1.71	0.47	0.14	1.41	1.59	–
VA [65]	One source of VA have been ground at different intervals of 30, 60, 90, 120 min[a]	20[b]	47.74	15.36	12.88	8.25	6.45	3.62	1.11	0.66	40-
		5[c]									–
		2.5[d]									52
		3[e]									40

[a] Chemical composition before and after the treatment has not been measured.
[b] Original.
[c] after 30 min milling process.
[d] after 90 min milling process.
[e] after 120 min milling process.

However, in dissolution tests, Fig. 3d, FA particles dissolve fully, and only crystal structure of cenospheres and un-reactive particles remain.

It is important to note that the formed layer on the particle surface does not stop the dissolution entirely but reduces it significantly. This can be elucidated from the slow rate of mechanical strength development over time [28,56].

4.2. Reactivity of precursors

In Section 4.1, it was demonstrated that the particle size distribution of the aluminosilicate source influences the setting time. Next to this, the reactivity of the used solid precursor has been reported as another important parameter that influences the setting time and resulting strength. This reactivity can be influenced by thermal [28,70], mechanical [55,62], or chemical treatments, see Fig. 4 [71]. The importance of each method is explained in the following sections.

4.2.1. Thermal activation

A well-known example of thermal activation of aluminosilicates is the calcination, and consequently dehydroxylation, of kaolin to produce metakaolin. During heating, less-reactive kaolin is transformed into highly-reactive metakaolin by changing the crystalline structure to disrupted layered structure [77]. There is a fundamental premise upon this transformation that the aluminum coordination number changes from 6 to a mixture of 4, 5, and 6 due to thermal dehydroxylation [78,79]. However, this dehydroxylation is partially reversible when metakaolin rests at a humid environment [30,77–80]. Furthermore, the calcination temperature is significantly important and has an optimum at about 700 °C [70]. Temperatures above or below this point delay the geopolymer setting time, as shown in Fig. 5a [70]. This is explained by the fact that under-calcined material is not fully disordered while over-calcined material begins to sinter and partially recrystallize. Notably, the maximum compressive strength has often been obtained by metakaolin with the fastest setting time, see Fig. 5a [70]. Besides the role played by the calcination temperature, the calcination rate is another significant parameter in the thermal treatment of aluminosilicate [81]. It has been clearly observed that by raising the rate of calcination of kaolin from 1 to 20 °C/min to reach a maximum calcination

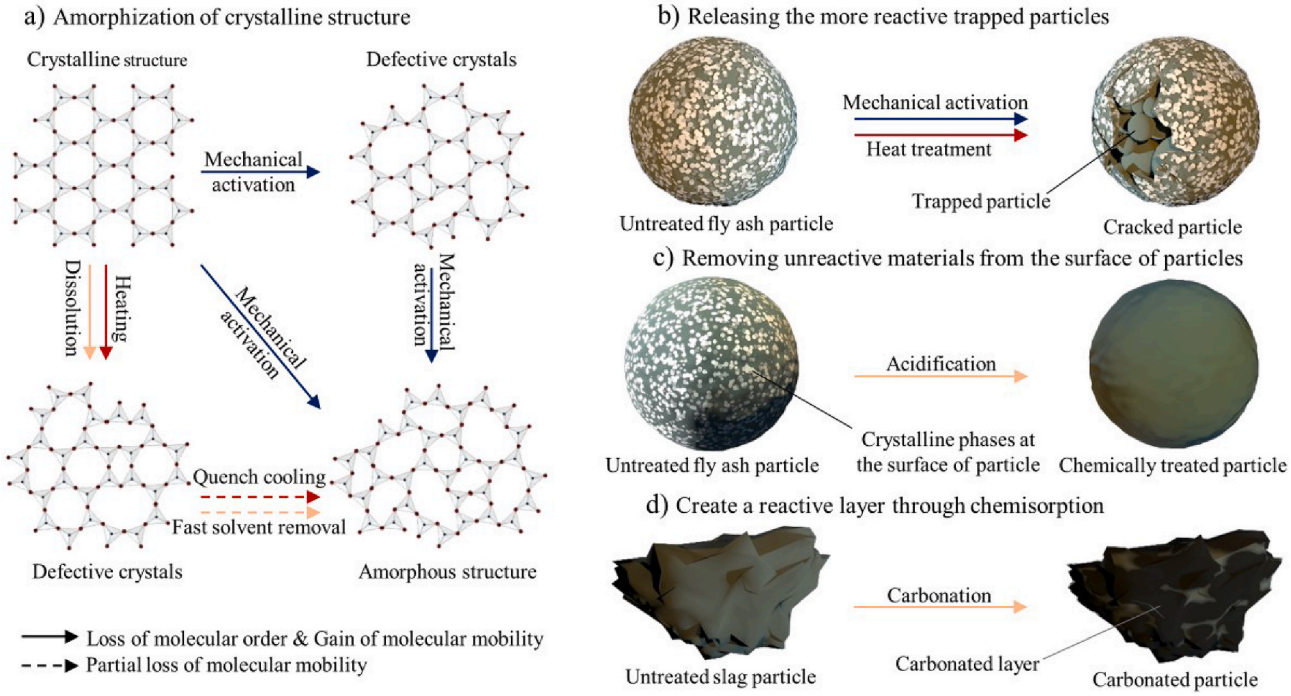

Fig. 4. a) Ideal schematic of different approaches of amorphization; b) releasing of more reactive materials trapped at larger FA particles through mechanical or heat treatments; c) removing an unreactive crystalline layer from the surface of FA particle using acidification; d) producing a reactive layer through chemisorption of carbon dioxide. The concepts have been obtained from the Refs [28,58,64,72–76].

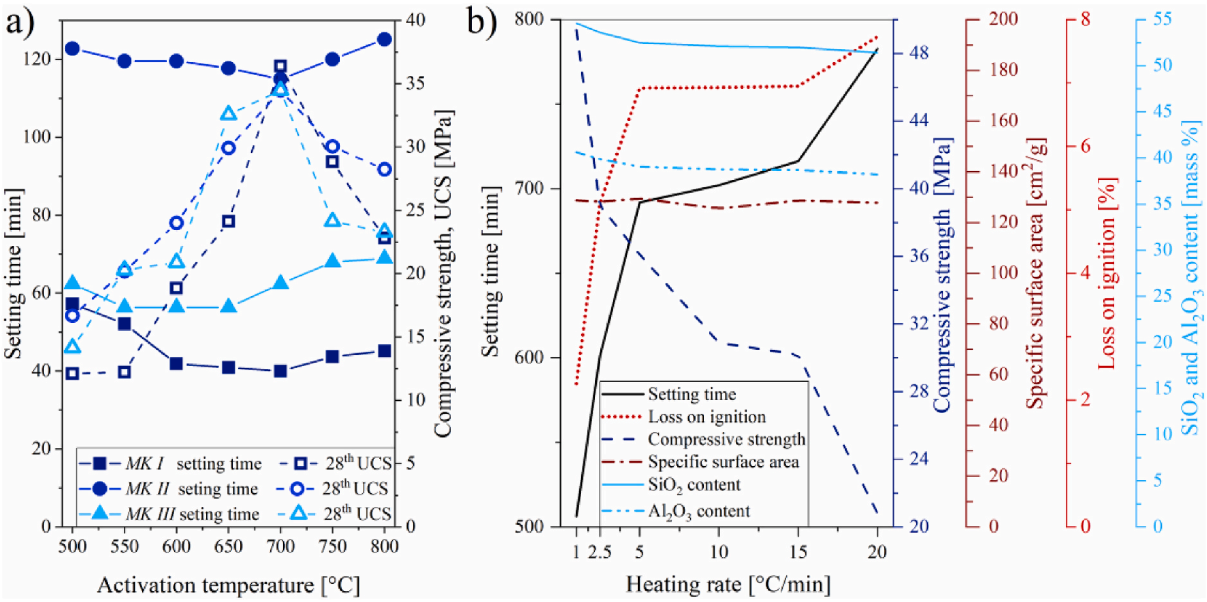

Fig. 5. a) Influence of activation temperature and b) calcination rate of kaolin on setting time and compressive strength of metakaolin based geopolymer. The data have been adapted from Refs. [70,81].

temperature of 700 °C for 30 min, the initial setting time of the corresponding geopolymer retarded from ~510 to 770 min, Fig. 5b [81]. This has been associated with the level of dehydroxylation of kaolinite and purity of the produced metakaolin, which is higher at a slower rate of heat evolution [81]. It is interesting to note that the particle size and specific surface area of the metakaolin calcined at different heating rates did not change. While the loss in ignition has been significantly reduced at the material with the minimum heating rate. Taking this loss into account, the mass is replaced with silicates and aluminates in slow rate calcined metakaolin geopolymer, which results in higher compressive strength, see Fig. 5b [81].

A similar trend has been observed for waste aluminosilicate products such as FA and palm oil fuel ash (POFA). For example, preheating of as-received FA and POFA to temperatures between 300 and 500 °C for 1 h resulted in ~10–20% acceleration in setting time of the corresponding geopolymers, while extending the preheating to 800 °C has a retarding effect on the setting time of both materials, Fig. 6a [28]. The significant delay in setting time of the material at 800 °C is due to the formation of a fully crystalline structure [28]. Besides, it is important to observe that the long-term compressive strength of untreated FA geopolymer and

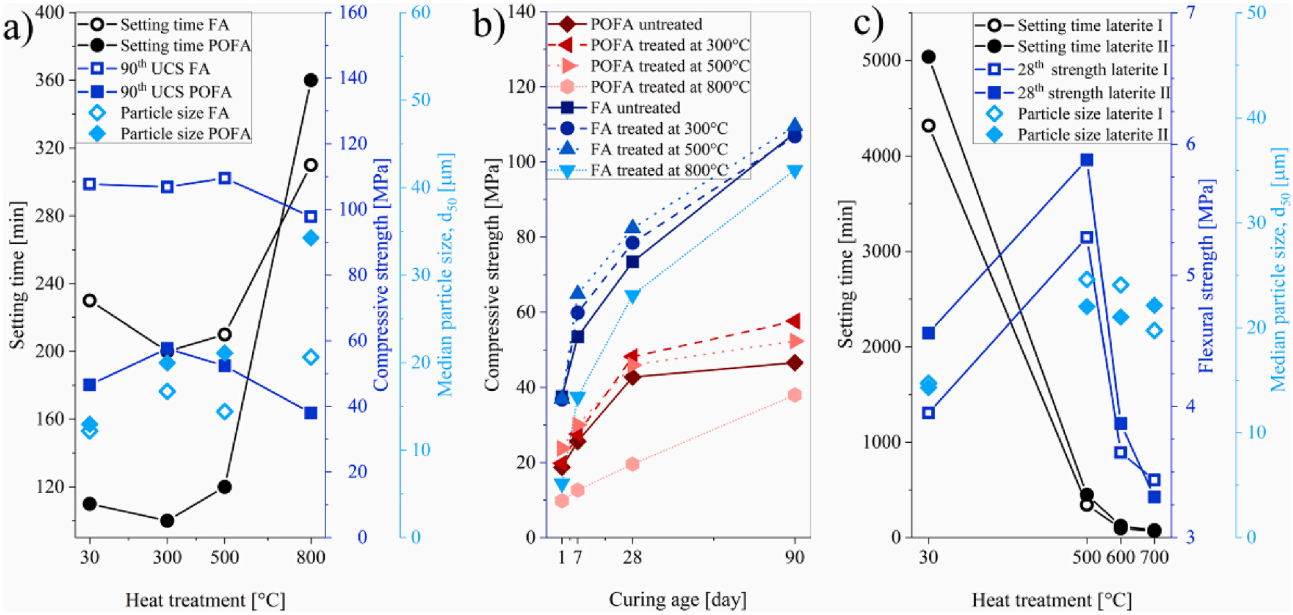

Fig. 6. a) Effect of heat-treatment on the setting, particle size and 90th-day compressive strength of FA and POFA; b) compressive strength of FA and POFA based geopolymer over time; c) effect of heat-treatment on the setting, particle size and 28th-day flexural strength of iron-rich aluminosilicate source, laterite. The data have been adapted from Refs. [28,71].

Table 2
Effects of heat treatment sequence of FA on setting time of geopolymer. The data have been adapted from Ref [28].

Heat treatment protocol	Initial setting [min]	Final setting [min]	Particle size, d_{50} [μm]	Compressive strength [MPa]
As-received [Ref]	190	230	12	73 ± 3
Heated at 300 °C[a]	150	200	17	78 ± 3
Heated at 500 °C	160	210	14	82 ± 3
Heated at 800 °C	220	310	20	65 ± 10
Pre-dried at 110 °C[b]	170	220	12	70 ± 3
Pre-dried at 110 °C + heated at 300 °C	160	210	12	70 ± 3
Pre-dried at 110 °C + heated at 500 °C	160	220	12	71 ± 3
Pre-dried at 110 °C + heated at 800 °C	240	340	16	34 ± 7
Soaked[c] + heated at 300 °C + cooled at air	140	190	18	85 ± 4
Soaked + heated at 500 °C + cooled at air	130	180	18	93 ± 4
Soaked + heated at 300 °C + quenched at water	150	190	18	94 ± 4
Soaked + heated at 500 °C + quenched at water	140	180	21	96 ± 4

[a] all heated for 1 h.
[b] all pre-dried for 24 h;[c] all soaked for 24 h; resolution of setting measurement is 10 min for all.[d] The compressive strength is an average of at least three samples, which cured at 65 °C for 24 h and then cured for 56 days in ambient temperature before testing. All the materials activated using a similar activator type with identical liquid to binder ratio.

those treated up to 800 °C is almost similar. However, the development of the strength over time is different, see Fig. 6b [28]. This indicates that over time, the aluminosilicate source undergoes a further dissolution, and the chemical structure is continually changing. This is in agreement with the theory described in Section 4.1.

Likewise, an accelerating effect of heat treatment on the setting of geopolymers has also been reported for iron-rich aluminosilicates. For instance, calcination of laterite containing hydroxylated minerals at 500–700 °C has accelerated the initial and final setting time up to about 83 and 77%, respectively, Fig. 6c [82]. However, for this material, the optimum mechanical strength at 500 °C has not followed the setting time trends. This has been linked to the formation of the crystalline structure due to the sintering of the iron-rich aluminosilicate sources, which causes a lack of amorphous and disordered phases to form a binder gel. Comparably, an increase in the dissolution of reactive Si and Al of Fe-rich Bayer red mud has been reported by increasing the calcination temperature in the range of 200–800 °C, while it has been shown to reduce when calcined at 1100 °C [71].

Furthermore, the pre-treatment, heating, and cooling sequence is another factor influencing the thermal amorphization of aluminosilicates, Fig. 4a and b. Different heating protocols have shown that FAs which has been first soaked in water, heated up to 300–500 °C, and cooled down in air or quenched in water have the most accelerated initial and final setting times compared to the corresponding as-received and not soaked FAs, as shown in Table 2 [28]. It is interesting to note that this faster setting time has been observed while the particle size increased. This is due to the formation of micro-cracks on the FA particles during the fast water evaporation, which exposes more reactive materials to the activation environment, Fig. 4b [28].

4.2.2. Mechanical activation

The dominating effect of mechanical activation on improving the reactivity of aluminosilicate particles by increasing the specific surface area was discussed in Section 4.1. However, some studies have highlighted a kind of crystal structure disordering of minerals in a way to increase amorphousness of the aluminosilicates, such as FA [58,64,83,84], metakaolin [85], volcanic ash (VA) [65], and slag [86], without altering their chemical composition during the course of mechanical

activation. This has been often argued based on broadening the XRD peaks and lowering their intensities as indicators for amorphization in ground materials [55,58,64,85,86]. Considering these results, the mechanical activation process might be also considered as a way of increasing the chemical reactivity of aluminosilicates. This would be through two phenomena:

1. Triggering physicochemical changes and amorphization by the accumulation of mechanical energy for molecular disordering and increasing the molecular mobility, see Fig. 4a [64]
2. Exposing the more reactive fraction of the material to alkali activator, Fig. 4b [58,73].

These phenomena are depending on grinding energy and grinding time. When low grinding energy is introduced in the system, no grinding effect is observed. This is because the kinetic energy of the milling beads is not sufficient to initiate the milling process, e.g., grinding of FA using lab-scale stirred media mill for up to 10 min has shown no change in amorphousness of the material [64]. When the energy input is increased, the first de-agglomeration occurs, and with further increment in energy, the particles are ground finer, Fig. 7a. To note, grinding is very process dependent, e.g., different grinding energy has been observed for FA when different mills are used, and consequently, FAs with different particle sizes and specific surface areas have been yielded, Fig. 7b [64].

Next to the reduction of particle size, some studies have reported a weak tracking of reactivity enhancement of ground aluminosilicates using XRD, e.g., it has been shown that a 90 min mechanical activation of VA manifests itself as a decrement in crystallinity by ~60%, and speeds up the initial and final setting times of the geopolymer by more than 95% and 80%, respectively [65]. While, surprisingly, the crystallinity of the material was increased when it ground further to 120 min. This has been correlated to the recrystallization of glassy phases, Fig. 7c [65]. Another example is that grinding of FA using an eccentric vibratory mill for 60 min has not shown a significant influence in XRD

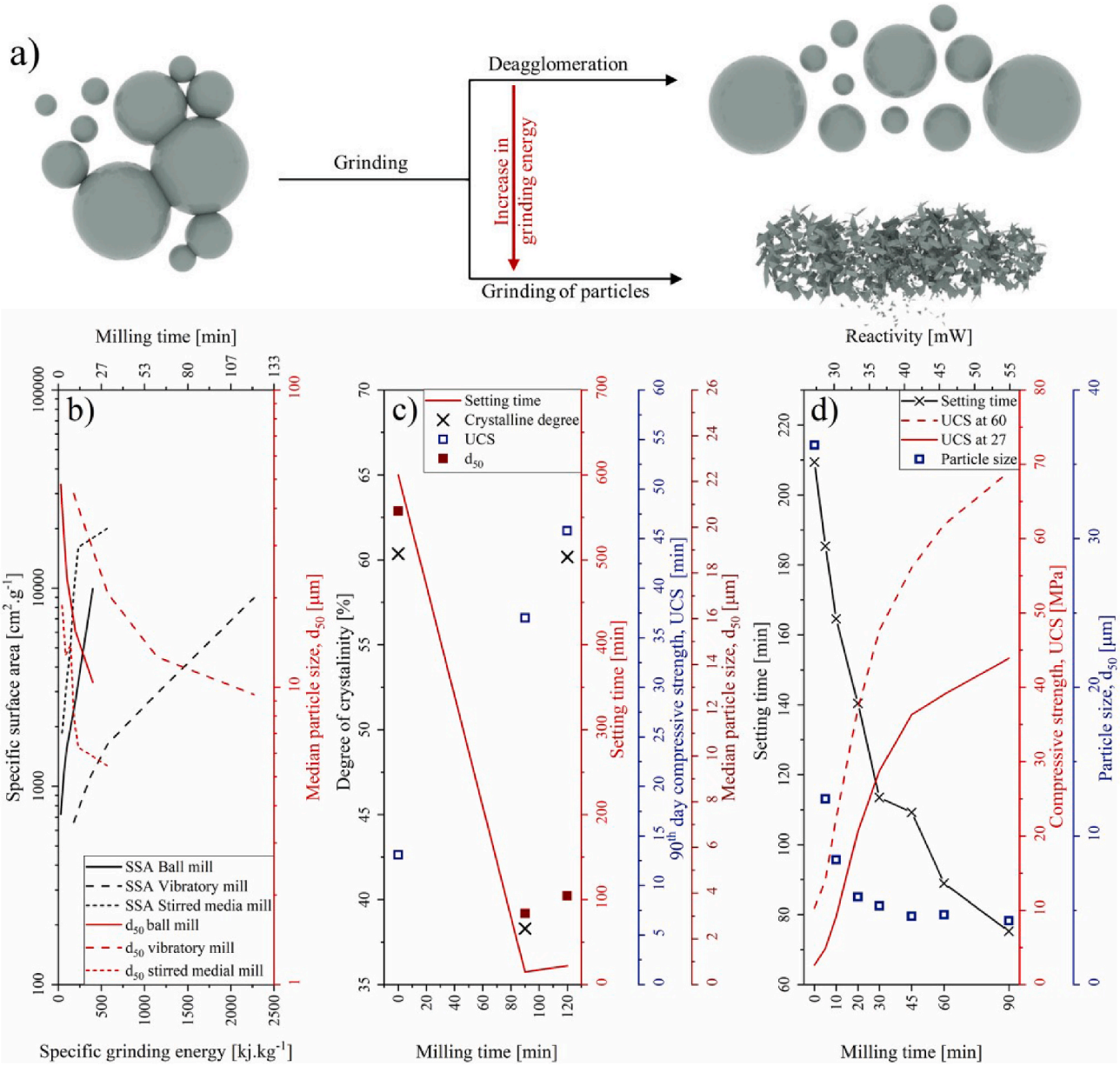

Fig. 7. a) Schematic effect of grinding energy on particles; b) correlation between grinding time and specific grinding energy on specific surface area and median particle size using three different mills; c) effect of grinding time on the degree of crystallinity, setting time and compressive strength of VA; d) correlation between milling time on particle size, reactivity, setting time, and compressive strength. The data have been obtained from Refs [55, 64, 65, 67].

patterns of milled particles, while further milling to 90 min showed a slight decrease in intensity peaks together with broadening quartz and mullite as damage in crystalline structure and particle breakage [55]. However, interestingly, an increase in the maximum peak of isothermal conduction calorimetry of milled FA has been observed. Taking this maximum value as an index to show the reactivity of the particle, it can be observed that increasing the milling time to reduce the particle size, increases the reactivity of particles, and consequently, accelerates the setting, and increases the compressive strength. Furthermore, these correlations are independent of the curing temperature, see Fig. 7d [55].

4.2.3. Chemical activation

Another method for increasing the reactivity of aluminosilicates is by chemical activation [74, 71, 75, 76]. Here two main mechanisms have been proposed:

1. Removing the impurities, Fig. 4c [74]
2. Producing a reactive layer on the surface of particles to facilitate the primary reaction, Fig. 4d [75, 76].

This activation mechanism is mainly proposed for waste materials because they are often disposed of in landfills without protection. There, they undergo a weathering process that results from the cyclic alteration in temperature and humidity. Additionally, depending on the chemical composition and storage environment, the surface of the particles can go through unwanted reactions and become covered with thin crystalline phases such as portlandite, gypsum, calcite, sodalite, and domilite [39, 74]. By removing these impurities, the reactivity of the waste material increases. A possible removal way is by acidification, e.g., sodalite is washed by hydrochloric acid [74]. However, it needs to be taken into account that high acid concentration not only dissolves the crystalline phases but also the glassy fraction of the material [38, 87, 88].

Another method is by coating the particles with a more reactive layer or by weakening the existing structural bonds [75]. For example, by chemisorption of CO_2 on ground slag, a highly reactive coating layer is formed on the surface of particles that increase interaction with alkali activators compared with the samples which have been processed in the air [75]. On the other hand, alkali-thermal treatment of red mud using Na_2O has been used effectively for phase transformation of sodium aluminosilicate hydrate into nepheline and peralkaline aluminosilicate phases, resulting in a higher dissolution of Al_2O_3 and SiO_2 in alkaline solutions. This has been attributed to the decrease in binding energies of Al–O and Si–O bonds due to the damaging of aluminosilicate structure, Fig. 4a [71]. In a similar manner, partially breakage of bonds of three-dimensional networks of glassy phases of FA have been correlated with higher reactivity of the material when it is activated with sodium hydroxide solution [76].

4.3. Chemical composition

It is widely accepted that the chemical composition of the aluminosilicate precursors influences the setting time and mechanical properties of the corresponding geopolymers. This makes the comparison difficult for pure precursors, and even more complicated for waste materials.

For pure precursors, it has been demonstrated that similar final mechanical properties can be obtained by adjusting the molar Si/Al ratio when the reactivity and particle size of the aluminosilicate precursors is similar [38]. If the particle size distribution is not similar, different final mechanical properties are expected, as explained in Section 4.1. Obtaining similar mechanical properties has not been shown for waste materials due to unknown reactivity, heterogeneity, and contamination [38, 69]. Despite this drawback, it is still possible to identify trends caused by the chemical composition.

4.3.1. Influence of Si and Al ions

The influence of Si and Al can be discussed on microscopic and macroscopic levels. The microscopic level investigates the interactions of molecules mainly using NMR or ICP, whereas the macroscopic level can be measured through setting time or mechanical properties. Both levels are important and cannot be viewed individually.

4.3.1.1. Microscopic level. The microscopic level considers more the reaction kinetics rather the mechanical properties. Here, two types of reaction kinetic needs to be considered: 1) dissolution of aluminate and silicate and 2) condensation reaction between both species and the formation of a three-dimensional aluminosilicate network [34, 89, 90]. Different rates of dissolution combine with the different tendencies of monomers influence the formation of further oligomers, which consequently affects the whole polycondensation at different stages of the reaction. For the dissolution of aluminate and silicate, it can be stated that aluminate has a faster initial dissolution rate, and is more soluble than silicate at a constant pH and low temperatures, such as room temperature [32, 91, 92]. In this line, for a geopolymer system with high Si/Al (molar ration of Si/Al>3), a prompt condensation between aluminate and silicate species has been suggested based on Si-NMR data [92], while for the further reaction between silicate species, a slow condensation reaction has been proposed [91]. However, at low Si/Al (molar ratio of Si/Al<1) system, the retard presence of silicate monomeric species suggests a rapid condensation of silicate units with $[Al(OH)_4]^-$ to generate aluminosilicate species. While the larger oligomers develop through subsequent condensation with the lately released $[Al(OH)_4]^-$ to build-up of aluminosilicate networks gradually [31]. This statement is supported by reaction enthalpy data shown in Table 3 [93]. From this table, it can be seen that a reaction between silicate and aluminate is the most preferred reaction, followed by aluminosilicate with another silicate. It is worth to note that, apart from the clear tendency of silicate in aluminate, there is also a priority on reaction rate among different silicate species, and some are more reactive than others. For example, considering the two possible stable silicate species of $[SiO_2(OH)_2]^{2-}$ and $[SiO(OH)_3]^-$, the latter has been registered for a higher possibility to condense with $[Al(OH)_4]^-$ [31].

4.3.1.2. Macroscopic level – Si and Al from solid sources. The influence of silicate and aluminate from solid sources on the macroscopic level is shown in Fig. 8. There, various precursors have been replaced with a Si-rich material, such as rice husk ash and nano-silica, to increase the silicate content in the system [94–97]. Details to each system are shown in Table 4. Independent of the initial precursor and the second source, it can be seen that an increasing silicate amount in the system delays the setting time, Fig. 8a. This effect is also independent of the curing temperature [97]. The observed delay in setting time can be explained by phenomena at the microscopic level, as previously mentioned. As shown in Table 3, the speed of the condensation reaction of two silicate species is slower due to a lower reaction enthalpy compared to a combination of aluminate and silicate. This means that with increasing silicate content in the solution, the reaction rate of the whole system is reduced. As a result, the setting time increases. Next to this, the higher silicate content decreases the compressive strength, Fig. 8b. This decrease is probably due to two effects: a) increasing of the dissolved silicate concentration results in an unstable geopolymer gel [98] and b) the formation of less binder, here reactive aluminosilicate, in the system. For the shown data,

Table 3
Calculated energies for different condensation reaction [93].

Reactions		Energy [kcal mol^{-1}]
$Si(OH)_4+[Al(OH)_4]^-$	$\rightarrow [SiOAl(OH)_6]^-+H_2O$	−27,0
$[Si_2O(OH)_6]+[SiOAl(OH)_6]^-$	$\rightarrow [SiO_3AlO_4(OH)_8]^-+2H_{2O}$	−11,3
$2Si(OH)_4$	$\rightarrow [SiO(OH)_{6]+}H_2O$	−4,9
$2[Si_2O(OH)_6]$	$\rightarrow [Si_4O_4(OH)_8]+H_2O$	−2.8
$2[Al(OH)_4]^-$	$\rightarrow [Al_2OH(OH)_6]^-+OH^-$	41,1
$2[Al(OH)_4]^-$	$\rightarrow [Al_2O(OH)_6]^{2-}+H_2O$	53,0

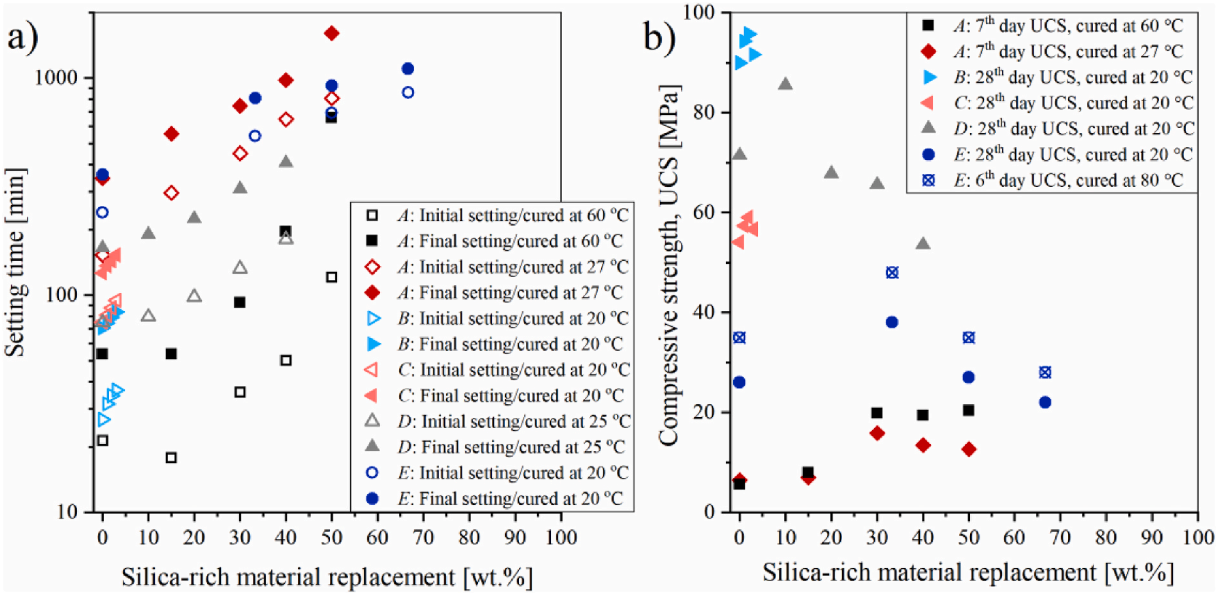

Fig. 8. Effects of silicate concentration on a) initial and final Vicat setting time and b) compressive strength of geopolymers. The data have been collected from Refs [94–97].

Table 4
Oxide composition of the aluminosilicate sources presented in Fig. 8.

Sample	Material	Remarks	SiO_2	Al_2O_3	Fe_2O_3	CaO	MgO	Na_2O	K_2O	Median particle size [μm]
A	Calcined water treatment sludge	R[a]	58.99	24.64	6.63	0.69	1.14	4.08	1.52	13.2
	Rice husk ash [97]	S[b]	89.17	0	0.41	0.61	1.22	7.29	1.12	13.7
B[c] & C[d]	Slag	R	34.44	13.31	0.47	37.42	9.89	0.34	0.47	12.4
	FA	R	54.62	24.42	7.21	4.44	1.43	0.73	1.75	22.1
	Nano-silica [96]	S	98.68	0.37	–	0.09	–	0.32	0.35	0.1
D	MK	R	55.87	42.25	0.38	0.04	0.04	0.26	0.31	5.9
	FA [95]	S	55.86	31.74	3.28	1.67	0.39	0.42	1.15	22.3
E	MK	R	55.57	41.55	0.54	0.04	0.05	0.26	0.43	7.9
	FA [94]	S	54.77	27.28	4.31	3.49	0.61	0.62	1.42	30.6

[a] R: Reference material.
[b] S: substitutive material.
[c] mixture of 70 wt% slag and 30 wt% FA as the aluminosilicate sources.
[d] mixture of 30 wt% slag, and 70 wt% FA as the aluminosilicate sources.

aluminosilicate sources have been replaced with solid silica sources, meaning the reactive aluminosilicate is reduced.

4.3.1.3. Macroscopic level –Si/Al from solid sources and further Si from liquid sources. As shown in Fig. 8, the setting time and compressive strength are influenced when aluminosilicate sources are substituted with solid Si-sources. Another method to alter the silicate content in the final geopolymer system is by the addition of silicate as a solution. In this case, an alkaline silicate solution (such as sodium silicate and potassium silicate) is used next to strong alkaline hydroxide (such as sodium hydroxide and potassium hydroxide) to increase the silicate content in the final mixture and to control the mechanical properties [31, 98]. The silica supplied through an alkaline silicate activator is more reactive compared with those supplied through solid sources and reacts quicker with the released aluminate [92,99]. Therefore, it is an important controller of the geopolymer setting time.

Fig. 9a and b show the influence of added sodium silicate and sodium hydroxide on the setting time and strength [100–103]. For a better comparison, data have been converted into SiO_2/Na_2O ratio. Fig. 9a and b show an acceleration of setting time when more sodium silicate is available in the solution [100–103]. Of interest is that both figures show that the setting time as a function of SiO_2/Na_2O passes a minimum value. In Fig. 9a, the minimum is at a SiO_2/Na_2O mass ratio of ~2, whereas when molar ratio is used, the minimum shifts to around ~1.5. This shift is due to the presentation of the data. When the mixing design is expressed in a mass ratio, the increase of silicate/hydroxide solution not only increases the silicates of the system but also reduces the water content as the density of silicate solution is higher than those of hydroxides. Therefore, as the side effect of variation in water content is eliminated in the molar calculation, an optimum value for the influence of silicates and hydroxide is more visible [101,103–105]. The influence on the setting time by altering the SiO_2/Na_2O content has been associated with the faster dissolution of the precursors in more alkaline environments as the presence of OH^- enhances the solubility of silica and alumina [105,106]. The compressive strength, on the other hand, increases with increasing silicate content, and after reaching a maximum it decreases again, as shown in Fig. 9a–c. This trend in strength is independent of the precursor and has been expected [98,107]. At low SiO_2/Na_2O ratios, the available silicate is insufficient to react with all $Al(OH)_4^-$ anions. Hence, the silicate needs to be supplied from the solid sources with a lower rate of reaction. As a result, the maximum strength is not reached. With increasing the silicate solution, all the available $Al(OH)_4^-$ anions react with the silicates, and maximum strength is obtained. Once the concentration of silicates is high in the solution, as the Si/Al ratio is significantly increased, the gel structure becomes unstable, and the strength decreases again, as discussed at the microscopic level in

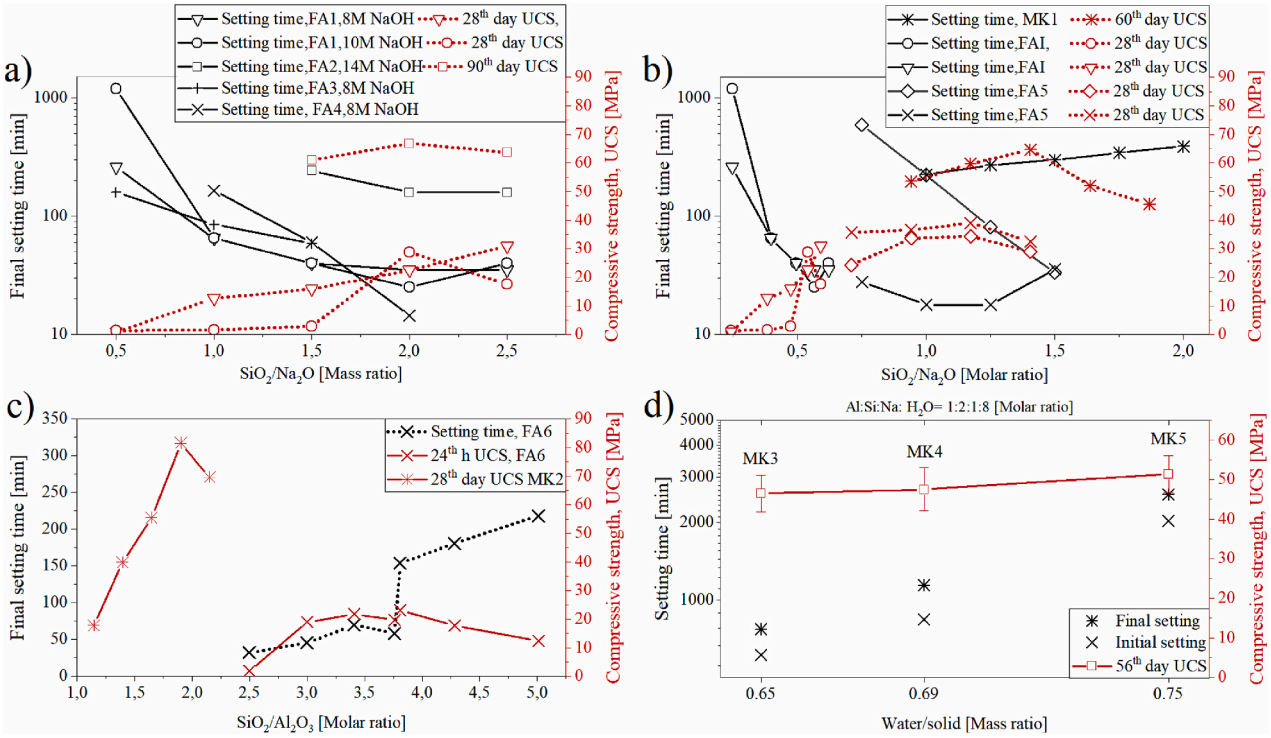

Fig. 9. Effects of added silicate as sodium silicate to sodium hydroxide solution in a) mass ratio; b) molar ratio on final setting and compressive strength of different FA based geopolymers; c) effect of Si/Al molar ratio on compressive strength of the FA and MK based geopolymers; d) adjustment of the molar ratio of MK based geopolymer for final mechanical strength. The data have been adapted from Ref. [38,98,100–104,107,108]. Oxide composition, LOI, and particle size distribution of the used materials have been privided in Table 5.

Section 4.3.1.

The role of silicates in the solution form has been investigated from another view by adjusting the final molar Si/Al ratio of three different MK based on known reactivity of aluminosilicate precursor using sodium silicate solution. The result has shown that the setting time is influenced but the final compressive strength is not, as shown in Fig. 9d [38]. This variation in setting time is due to the existence of different sources of silicate in the systems (viz. dissolved silicate, and those in solid form). In this regard, to obtain a molar Si/Al ratio of 2:1, either more or less liquid silicate has to be added, see the chemical composition in Table 5. It can be seen that when the metakaolin had a higher concentration of Si, the setting time is delayed. This delay is due to the fact that more Si has to be dissolved from the precursor. However, when the Si concentration in the precursor is lower, more silicate has to be added as the silicate solution, thus making it "ready" for the chemical reaction. Of interest is that the final compressive strength is similarly independent of the used precursor.

Table 5
Oxide composition, LOI, and particle size distribution of the material used in Fig. 9. The data has been adapted from [38, 98, 100–104, 107, 108].

Aluminosilicate	SiO_2	Al_2O_3	CaO	Fe_2O_3	LOI	Median particle size, d_{50} [μm]
FA1 [101]	52,3	38,6	0,7	2,9	1,4	–
FA2 [102]	53,7	27,2	1,9	11,2	0,7	–
FA3 [100]	46,0	33,0	2,6	10,5	–	20,0
FA4 [103]	39,8	17,9	15,5	15,0	0,5	–
MK1 [108]	59,6	38,0	–	–	0.5	–
FA 5 [104]	46,1	25,0	8,0	7,6	0,5	–
FA 6 [107]	46,0	33,0	2,6	10,5	–	20,0
MK2 [98]	–	–	–	–	–	–
MK3 [38]	42,0	35,0	–	–	1,0	6,5
MK4 [38]	56,0	38,1	–	–	0,8	5,4
MK5 [38]	53,0	43,8	–	–	1,0	4,4

Table 6
Oxide composition of the materials used in Fig. 10.

Aluminosilicate	SiO_2	Al_2O_3	Fe_2O_3	CaO	MgO	Others
FA1 [100]	46,0	33,0	10,5	2,6	–	7,9
FA2 [103]	39,8	17,8	15,0	15,5	6,5	5,4
FA3 [45]	59,9	24,7	6,3	2,0	1,9	5,2
MK [110]	54,4	38,4	1,3	0,1	0,2	5,6

4.3.2. *Influence of Na/K ions*

The data shown in this section are only focused on sodium and potassium-based activation solutions. These are the most common activators due to cost and availability.

As a main rule, it can be said that independent of the used activator type, sodium or potassium hydroxide, increasing the molarity of alkaline hydroxide leads to acceleration in setting time, as shown in Fig. 10a [100,103,109]. The accelerated setting has been associated with the fact that the aluminosilicates dissolve easier at higher alkaline environments as the presence of OH^- enhances the solubility of silicates and aluminates [105, 106].

Furthermore, at a constant concentration, there is a difference between alkali activators of different types, sodium- and potassium-based activators. A faster rate of hardening has been observed for sodium-based geopolymers compared with those of potassium [110], see Fig. 10b. This difference is mainly associated with the different charge densities of the activator ions, which cation-anion pair interaction becomes smaller when the cation size increases. This means the cation with a smaller size, Na^+, tends more to react with the small silicate oligomers such as silicate monomers and dimers, and therefore, higher mineral dissolution and faster setting occur in NaOH than KOH [111]. On the other hand, when the Na^+ makes pair formation with small silicate oligomers, it does not tend to pair with another silicate anion. This hinders the formation of larger oligomers. While the larger ion, K^+, has

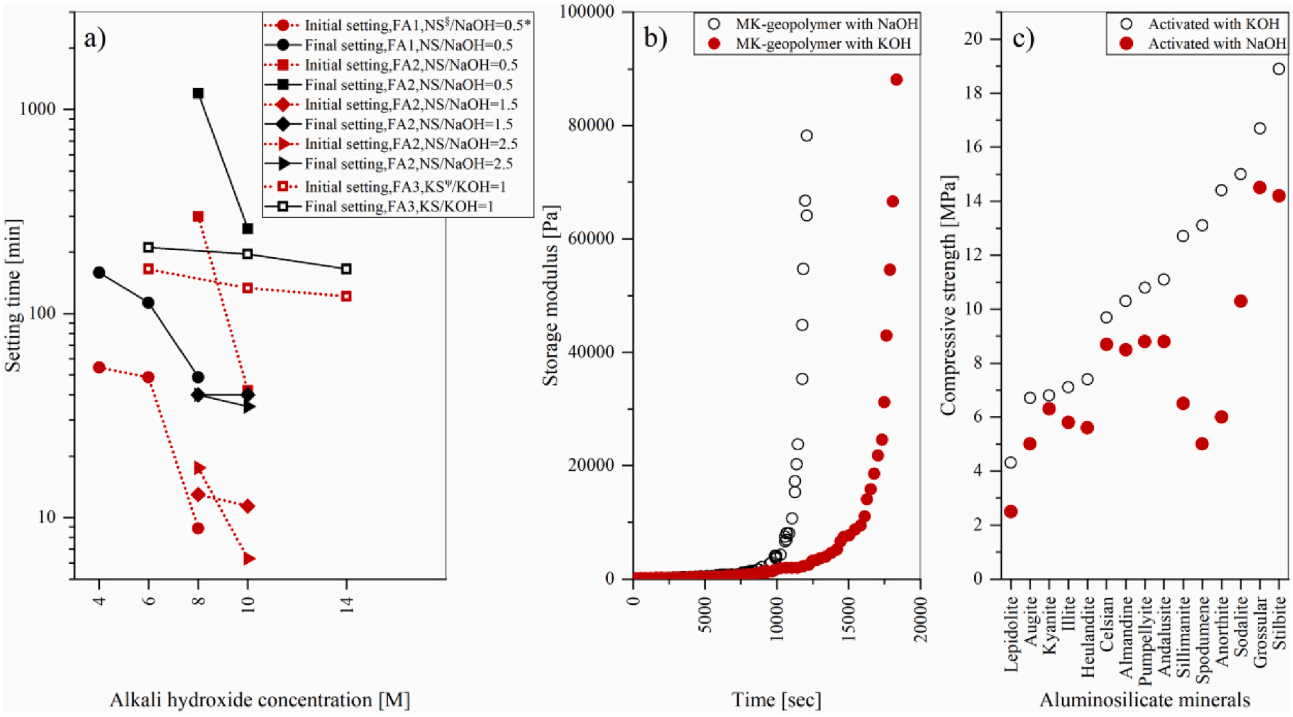

Fig. 10. Effect of a) activator content,* all in mass ratio; b) type of activator, sodium hydroxide or potassium hydroxide concentration on the setting time of geopolymers; c) comparison of compressive strength of different aluminosilicate minerals activated with sodium hydroxide or potassium hydroxide.[§] NS = sodium silicate; [Ψ] KS = potassium silicate; The data have been adapted from Refs [45, 100, 103, 110, 111].

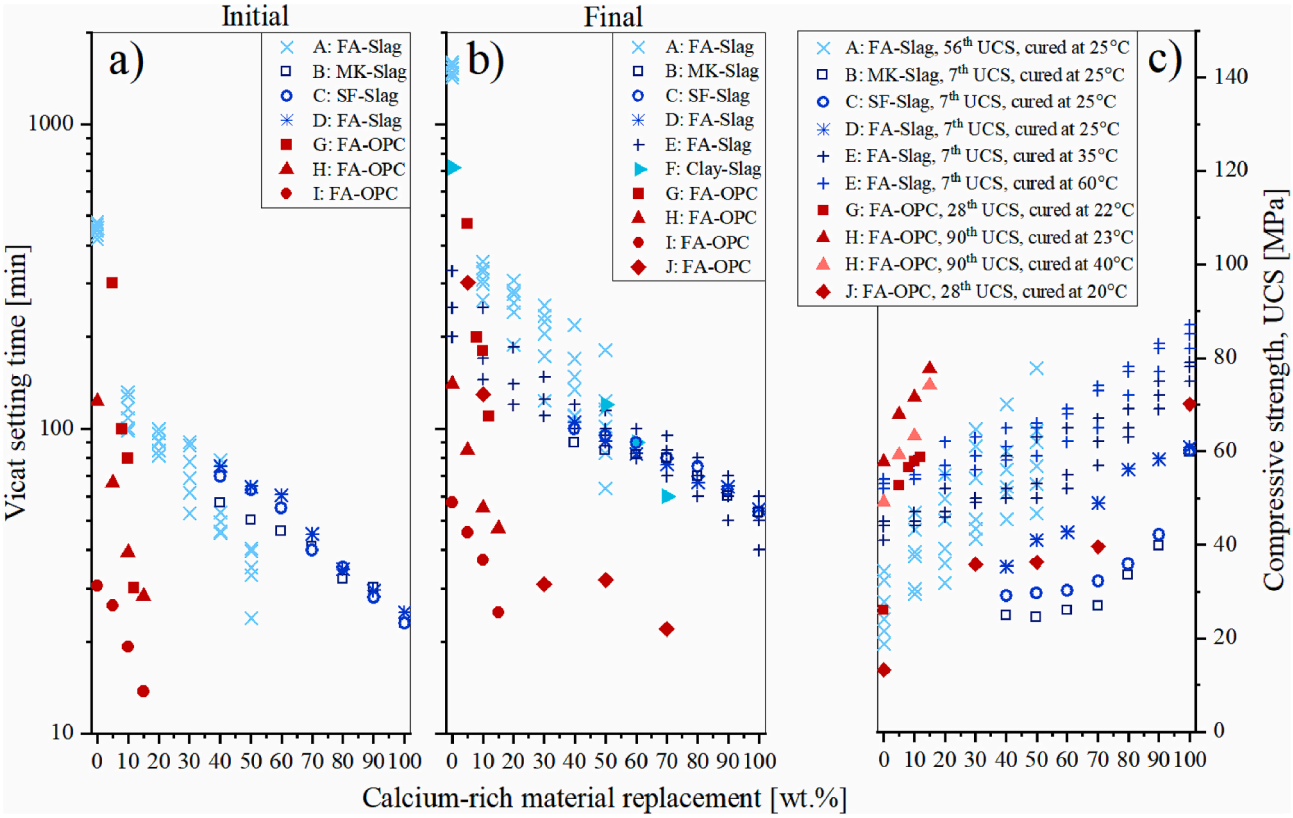

Fig. 11. Effect of Ca on a) initial and b) final setting time of different geopolymer matrices; c) compressive strength of geopolymer with the different replacement of Ca-rich sources. The oxide composition of all materials has been provided in Table 7. The data have been taken from Refs. [102,129–134].

less association with small silicate oligomers, and hence, tends to form larger oligomers that prefer to bind with aluminates [111]. Thus, it shows higher mechanical properties [110–113], see Fig. 10c.

4.3.3. Influence Ca ion

Apart from the basic elements of geopolymerization, Si and Al, it has been shown that calcium can act as a charge balancing cation like Na^+ and K^+, which results in a complex M_2O–SiO_2–Al_2O_3–CaO–H_2O system [114]. Calcium can be found as an inherent component of the waste aluminosilicates, e.g., high calcium FA and VA [115,116], or it can be added to a geopolymer system as an external source such as slag and OPC [117]. Depending on the pH of the medium and oxide concentration, the dissolution-precipitation reactions, and hence the stable equilibrium phase assemblages of the oxides, can be varied in different systems [118]. At a microscopic level, calcium can either precipitate as $Ca(OH)_2$ by lowering the alkalinity of the medium, and thus the driving force for dissolution of silicate and aluminate, or interfere with the formation of the geopolymeric gel by reacting with the dissolved silicate and aluminate species [119]. As a result of the latter interaction, the formation of C-A-S-H or C–S–H gel follows [120]. This formation does not occur solely but in coexistence form through C-A-S-H/N-A-S-H or C–S–H/N-A-S-H gels in the matrix [44, 118]. To this end, when low concentrations of alkali activator are present in a Ca-rich environment, it is expected that the formation of amorphous C–S–H gel dominates. However, when the concentration of hydroxides is high, the precipitation of $Ca(OH)_2$ will be promoted. Here, the precipitation of $Ca(OH)_2$ inhibits any possible formation of C–S–H gel in the geopolymeric binder unless a significant amount of calcium is presented initially [121]. This expectation has been demonstrated for MK-based geopolymers with incorporated $Ca(OH)_2$ [122].

At macroscopic level, fast setting has been measured by substitution of MK and Class F FA with Ca-rich sources, such as Class C fly ash [123, 124], slag [44, 124], oyster shell [40,125], calcium hydroxide [126], calcium silicate [119], and OPC [102,127]. Fig. 11 shows the Vicat needle setting time of different geopolymeric systems at the presence of two different Ca-rich sources, OPC and slag. The composition detail of the material can be seen in Table 7. Independent of the type of material, the replacement of Ca-rich sources accelerates both initial and final setting time of the material, as seen in Fig. 11a and b. Furthermore, it is notable that in cement substitution series much faster setting is observed, which probably can be linked to the precipitation mechanism, while having less Ca content in the slag substitution series results in a more gentle acceleration rate of setting. Interestingly, these trends have also been observed in the rate of compressive strength development of the geopolymers, Fig. 11c. With this regard, it has been discussed that geopolymer gel is the contributing component in a high alkalinity system, while when the alkalinity is low, the Ca-rich components are the dominant contributor to the strength [121]. On the other hand, depend on the mechanism of Ca participation in the whole reaction including the formation of amorphous C–S–H gel or precipitation of $Ca(OH)_2$, the Ca products can structurally increase the strength in the form of either strong micro aggregate or stronger binder product [44, 121]. Here, the reactivity and concentration of Ca in OPC particles suggest a higher efficiency in strength development when this material is used as a substitution rather slag, Fig. 11c. As discussed in Fig. 3b, there should be a cessation in the reaction of Ca-rich precursors, similar to aluminosilicates, and the partially reacted particles are always present in the system. These particles can densify the matrix as micro aggregates [44, 128]. Therefore, the reactivity of the material is again an important parameter here, not only to control the setting of material at an early age but also to control the final strength.

4.3.4. Effect of water

Next to the activator type and molarity factors, the alteration of water/solid content is another key parameter regarding the setting time and mechanical strength. This can be indirectly seen in Fig. 12a and directly in Fig. 12b and c.

Fig. 12a shows that by increasing the amount of activator, the setting time is delayed. This retarding effect is due to the additional water concentration in the system [102,135]. However, it is assumed that the altered setting time is not caused by a lower dissolution of aluminosilicates, but a reduction in viscosity of the system which cannot be detected using the Vicat needle apparatus. Regarding the mechanical strength, it is important to note that if the activator is less than a certain amount, several aluminosilicate precursors remain unreacted since the medium in which the reaction occurs is missed. Besides, the lack of sufficient water has always argued to be a reason for poor compaction of the matrix, which weakens the mechanical strengths [136,137]. For the provided data in Fig. 12a, it was assumed that the amount of activator is more than the minimum/optimum value. Correspondingly, the secondary effect of water that is induced by increasing the activator/solid ratio causes a reduction in compressive strength of the material [102, 138,139], which is mainly due to the formed porous structure [140].

The direct influence of water has rarely been discussed in the literature for geopolymers. However, similar to what has been observed for cement samples [141,142], with increasing the amount of water in the geopolymer paste, a delayed Vicat needle setting time is measured, Fig. 12b [136]. As discussed above, this is due to a viscosity change that

Table 7
Oxide composition of the aluminosilicate sources presented in Fig. 11.

Sample	Material	Remarks	SiO_2	Al_2O_3	Fe_2O_3	CaO	MgO	Na_2O	K_2O	Median particle size [μm]
A [129]	Fly ash	R[a]	58.90	32.24	2.84	0.73	0.89	0.35	1.12	–
	Slag	S[b]	32.57	16.98	1.26	34.07	9.69	0.20	0.08	–
B, C, D [130]	Metakaolin: B	R	52.21	44.08	–	1.69	–	–	–	–
	SF: C	R	85.76	1.89	0.56	0.92	0.81	0.74	0.86	–
	Fly ash: D	R	62.20	27.50	3.92	2.27	1.05	0.52	1.24	–
	Slag	S	32.40	14.96	0.83	40.70	5.99	0.42	0.29	–
E [131]	Fly ash	R	60.11	26.53	4.25	4.00	1.25	0.22	–	–
	Slag	S	34.06	20.00	0.80	32.60	7.89	–	–	–
F [132]	Clay based material	R	50.28	41.99	1.03	0.14	0.02	–	0.59	–
	Slag	S	22.38	8.09	2.31	37.44	3.51	–	1.26	–
G [102]	Fly ash	R	53.71	27.20	11.17	1.90	–	0.36	0.54	–
	OPC	S	21.10	4.70	2.70	63.60	2.60	0.50	–	–
H [127]	Fly ash	R	36.0	14.9	19.7	19.4	2.6	0.7	1.0	–
	OPC	S	20.8	4.7	3.4	65.3	1.5	0.4	0.1	–
I [133]	Fly ash	R	29.32	12.96	15.64	25.79	2.94	2.83	2.93	8.5
	OPC	S	20.80	4.70	3.40	65.30	1.50	0.10	0.40	14.6
J [134]	Fly ash	R	50.97	27.83	9.21	2.62	1.43	1.13	3.73	–
	OPC	S	12.22	3.85	2.85	73.82	0.73	–	1.17	–

[a] R: Reference material.
[b] S: substitutive material.

Table 8
Oxide composition, LOI, and particle size distribution of materials used in Fig. 12.

Aluminosilicate	SiO_2	Al_2O_3	Fe_2O_3	CaO	MgO	Others	LOI	Median particle size [μm]
FA4 [102]	53,7	27,2	11,2	1,9	–	6,0	0,7	–
FA5 [139]	60,0	28,0	2,5	2,5	1,0	6,0	2,5	–
MK1 [138]	44,9	50,9	0.8	0,1	0,1	3,2	1,0	3,6
Silica fume, SF [138]	92,4	0,7	0,8	0,4	1,0	4,7	1,7	12,5
MK2 [145]	59,5	34,0	–	–	–	6,5	1,1	2,9

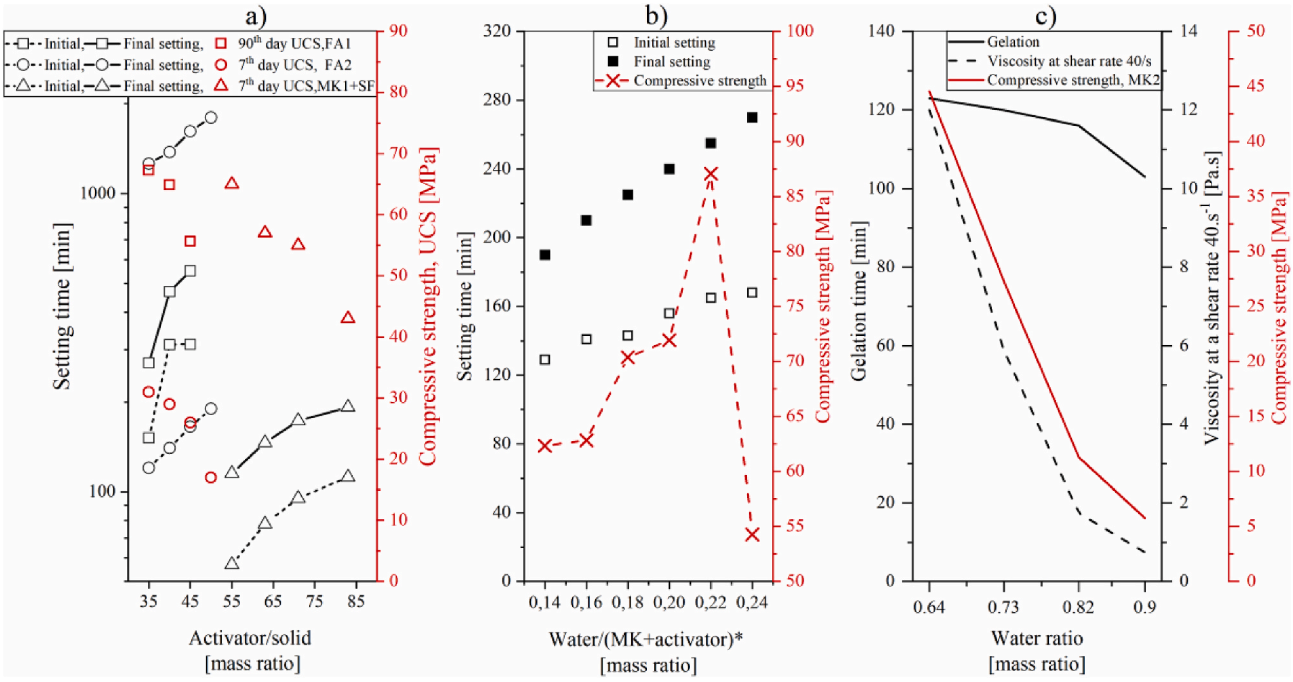

Fig. 12. a) Effect of activator content, and b) water content on setting and compressive strength of different geopolymers geopolymer; c) effect of water ratio on gelation time, viscosity, and compressive strength of metakaolin based geopolymer; * all composition are in mass ratio. The chemical composition of the materials has been provided in Table 8. The data have been adapted from Ref. [102,136,138,139,145].

cannot be measured by the Vicat needle [43]. Of interest is that when the setting time is measured by rheology, in particular oscillation measurements, the setting time is less dependent on the water concentration, see Fig. 12c. This behavior is expected because the water does not take part in the chemical reaction and is only the medium in which the reaction occurs [34,143]. Besides, these results confirm the assumption for Fig. 12a that the changes in setting time are not due to the lower dissolution of aluminosilicates. Despite this, as discussed above, higher water concentration causes an increased porosity, which in turn, reduces the mechanical properties of geopolymers [52,140,144]. Therefore, optimized water content has to be determined for every cementitious system.

5. Effect of curing temperature

The curing temperature influences the dissolution and reaction kinetics of geopolymers. As shown in Fig. 13, independent of activator types, the setting time can be significantly reduced for MK and FA based geopolymers when the curing temperature is increased from room temperature to 100 °C [35,146–148]. The chemical composition of each sample is shown in Table 9. In principle, this high rate of setting can be explained by temperature-controlled dissolution characteristics of aluminosilicate precursors that are more reactive at higher temperatures [42, 66]. Therefore, more material is available for quick condensation. In addition, if the sample is not covered, the evaporation of water is higher at high temperatures, which results in a higher concentration of the remaining alkali activator. This phenomenon increases the dissolution rate of aluminosilicate particles [42, 66]. It should be noted that the surface in contact with hot air is hardened earlier while the core is still in a fresh state; therefore, heterogeneities may occur in the sample [28]. Furthermore, this phenomenon can be a source of mismeasurement in setting using the Vicat needle [28].

Next to the acceleration effect on setting time, increasing the curing temperature influences the mechanical strength development of geopolymers. It has been widely accepted that curing geopolymers at higher temperatures results in high early strength of the material, while it has an adverse effect on the final strength [149]. This is clear in Fig. 13a as the gap between 1st and 7th days compressive strength is much lower when the material is cured at higher temperatures [146]. However, the rate of strength development at low-temperature curing is higher. Unfortunately, data for a longer curing age is not available for this study, but the higher rate of strength development when geopolymer cured at lower temperatures has been demonstrated in other studies, Fig. 13b [149,150]. This can be explained as at hot curing, both dissolution and condensation occur at a faster rate, therefore, more reactive material is available to condense, and high early strength is obtained. However, the fast process causes a large fraction of the aluminosilicates particles to remain partially reacted in the system with a very low rate of reaction afterward. This is due to the formation of gel products surrounding the particles that hinder the accessibility of solvent to inner layers of the particle on the one hand, and shortage of water in the system as the reaction medium, on the other [146,151]. In addition, curing at higher temperatures increases both the volume and size of pores. This has been correlated to the fast consolidation of material, which restricts the filling

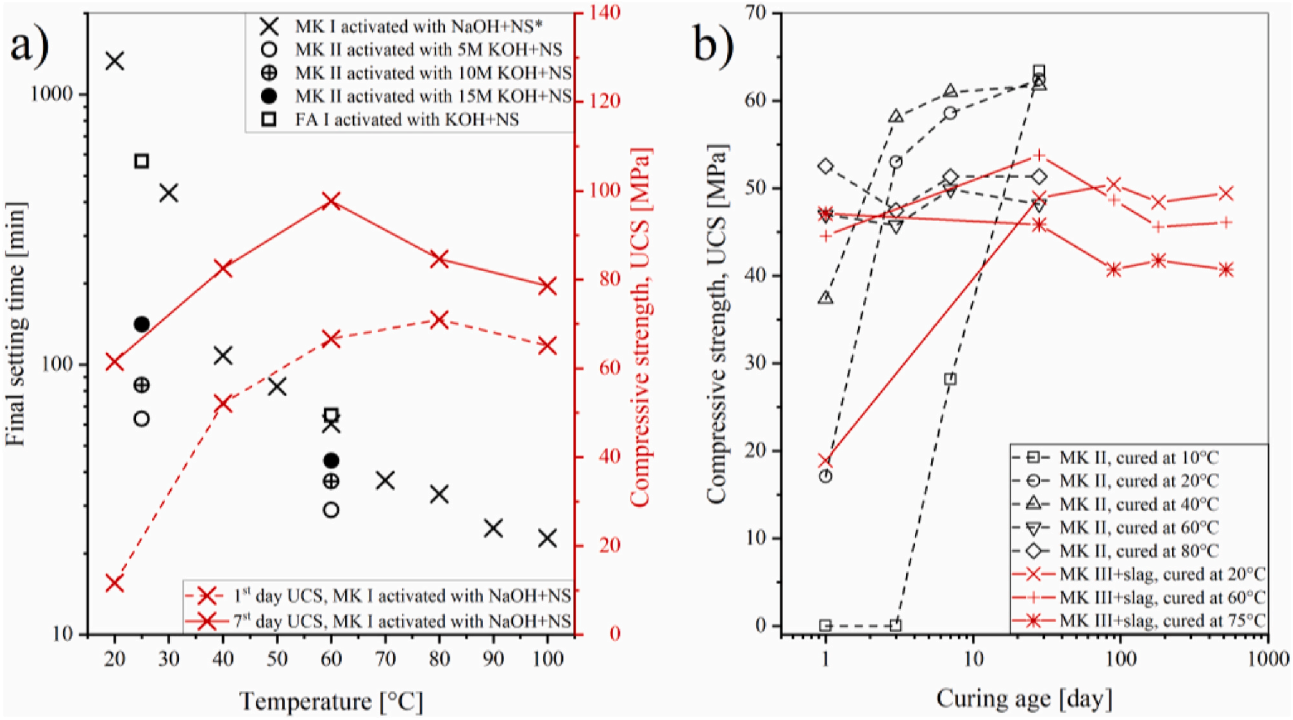

Fig. 13. a) Effect of curing temperature on the final setting time and compressive strength of different MK and FA based geopolymers; b) effect of curing temperature on the compressive strength of different MK based geopolymers as a function of time. * NS = sodium silicate. Data has been adapted from Refs [146–149, 151].

Table 9
Oxide composition of the FAs used in Fig. 13.

Aluminosilicate	SiO_2	Al_2O_3	Fe_2O_3	CaO	MgO	Others
MK I [146]	52,9	43,5	1,8	–	–	1,8
MK II [147]	52,3	42,8	1,0	–	–	3,9
FA I [148]	60,0	22,3	3,7	1,5	0,8	11,9
MK III [149]	40,9	55,0	0,6	0,1	0,3	3,1
MK IV [151]	51,1	45,3	0,3	0,1	–	3,2
Slag [151]	33,4	11,3	0,5	37,8	8,9	8,1

Table 10
Oxide composition of the FAs used in Fig. 14.

Aluminosilicate	SiO_2	Al_2O_3	Fe_2O_3	CaO	MgO	Others
FA I [123]	39,7	20,0	14,1	17,3	1,4	7,5
FA II [135]	49,8	27,7	7,1	3,9	2,7	8,8
FA III [155]	51,7	29,1	4,8	8,8	–	5,6

of pores [149, 151].

6. Effect of inorganic/organic additives

Several additives have been investigated to accelerate or retard the setting time of geopolymers. However, unwanted chemical reactions that occur between solid sources, activation solutions and additives make the geopolymer system more complex. Here, there are two main challenges. First, the additives have been often selected from those previously used in the cement industry. However, the performance of them in different cementitious systems should not be necessarily the same. As an example, it was found that calcium aluminate acts as setting time accelerator in OPC based materials [152] and FA based geopolymer activated using a mixture of sodium hydroxide and sodium silicate [135]. However, when calcium aluminate is mixed with sodium silicate solution, the setting is retarded [153]; Likewise, unlike what is observed in cement [154], the addition of citric acid in geopolymer has shown an accelerating effect on setting time [155]. Second, the ideal criterion of using additives is to control the setting time while maintaining the mechanical properties [123]. However, meeting such requirement is challenging, i.e., incorporation of 2.5 wt% citric acid or sucrose have accelerated and retarded the setting time of FA based geopolymer up to about 40%, respectively, while both of them were destructive to the ultimate strength of the material [155]. This means that a careful combination of admixtures is required to design a controllable system for a particular application. In addition, despite large databases available for cement, there is a limited number of studies available for different additives in geopolymers, Fig. 14 and Table 11. In the following, the important accelerators and retarders have been briefly explained.

6.1. Inorganic additives: alkali/earth alkali salts

6.1.1. Salts of single charge cations

Owing to the presence of intensive single charge cations form the alkali hydroxides solution in the geopolymer system, it has been suggested that the setting mechanisms of the geopolymer including salts of single charge cations are dominantly controlled by anions rather than the small fraction of induced cations from the additive [156].

6.1.1.1. Na-salts. It has been shown that the addition of 1–2 wt% Na_2SO_4 into a high calcium FA based geopolymer delays the initial setting but has no influence on the final setting time and the 7th-day compressive strength of the geopolymer paste [123]. This has been correlated to the formation of ettringite surround the aluminosilicate particles, which is a hindrance to the leaching of aluminates and silicates.

Using Na_2CO_3 as the activator of slag based geopolymer showed that Ca^{2+} ions from the dissolution of the slag react with those CO_3^{2-} of the activator and form initial calcium or sodium calcium carbonate. This reaction caused an increase in viscosity of the paste, while delayed the setting time of the material even to the point that no setting was measured within three days. This delay is due to the precipitation of

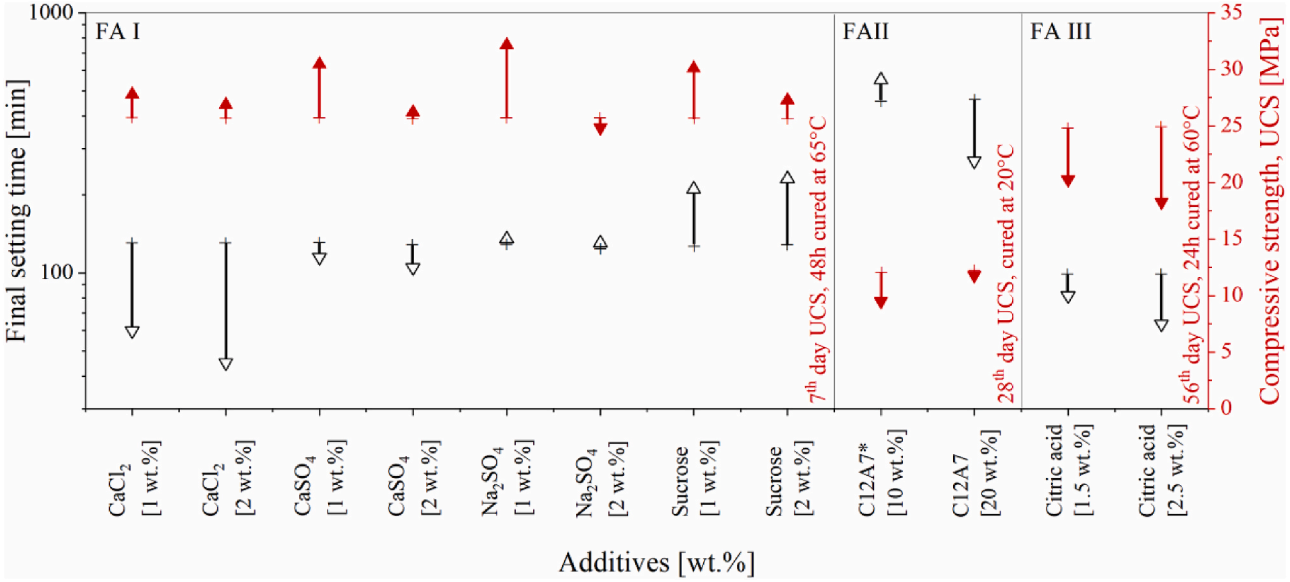

Fig. 14. Influences of different additive in setting time and compressive strength of different FA-based geopolymers. The plus (+) indicates the reference sample (geopolymer sample without additive), and the arrow shows the mixed geopolymer with additive. * Is dodecacalcium hepta-aluminate. The data have been adapted from [123, 135, 155]. Oxide composition of the FAs have been provided in Table 10.

Table 11
Influence of different additives on different geopolymeric systems. Oxide composition of the FAs and MK have been provided in Table 12. Data have been adapted from Ref [156].

Matrices	Final setting time [min]										
	Reference	KCl	K_2CO_3	KNO_3	$CaCl_2$	$Ca(OH)_2$	$CaCO_3$	CaO	$MgCl_2$	$Mg(NO_3)_2$	MgO
Mix1	62	153	88	95	56	58	–	40	–	–	–
Mix2	48	44	47	48	29	44	14	31	39	44	48
Mix3	67	67	69	67	43	64	30	49	67	65	67
Mix4	34	84	52	59	22	31	7	25	30	27	31
	7th-day compressive strength [MPa]										
Mix2	11	0	0	0	13	9	9	10	13	16	9
Mix3	36	39	45	42	37	35	47	58	41	43	35

Mixing compositions.
Mix1: FA1/MK = 2.02, activator/solid = 0.05, 15 M KOH/solid = 0.31.
Mix2: FA1/MK = 9.00, activator/solid = 0.18, 15 M KOH/solid = 0.28.
Mix3: FA2/MK = 9.00, activator/solid = 0.22, 15 M KOH/solid = 0.28.
Mix4: FA2/MK = 4.00, activator/solid = 0.08, 15 M KOH/solid = 0.35.
Note: dosage of additive for KCl, K_2CO_3, and KNO_3 is 0.08 M, for the rest additive the dosage is ~0.09 M.

Table 12
Oxide composition of the FAs and MK used in Table 11.

Aluminosilicate	SiO_2	Al_2O_3	Fe_2O_3	CaO	MgO	Others
FA I	48.5	29.6	4.6	6.1	2.3	8.9
FA II	50.0	28.0	12.0	3.5	1.3	7,8
MK	54.5	29.4	1.4	0.2	0.2	14.3

calcium carbonate on the anhydrous slag particles and builds a barrier that retards the progress of the subsequent reaction of the slag [106].

6.1.1.2. K-salts. The addition of KCl, K_2CO_3, and KNO_3 have shown that the performance of each is very dependent on the silicate concentration in the geopolymer matrices and can be either neutral or a retarder, Fig. 14 and Table 11. Interestingly, the compressive strength of different matrixes with these additives has not followed the setting behavior, i.e., despite additives were almost ineffectual in changing the setting of the geopolymers Mix2 and Mix3, the compressive strength of Mix2 was reduced to nearly zero, while the compressive strength of Mix 3 was not affected [156].

6.1.2. Salts of double charge cations

When the salts of double charge cations, such as Mg- and Ca-salts, are introduced to an alkaline solution, immediately metal hydroxides are formed, and consequently, hydroxyl ions are removed, therefore, a local pH drop occurs. This initiates polymerization and gelation if the silicate concentration is about to the saturation level. The total product of such a reaction has a low energy surface, due to the large particle size and small curvature, which enhance the conditions for coagulation upon collisions between the soluble silicates and the solid particles. Therefore, heterogeneous nucleation occurs through the matrix, which accelerates the hardening evolution of the matrix [156].

6.1.2.1. Ca-salts. In general acceleration in setting time and increase in strength have been often observed when Ca-salts have been used as an additive in geopolymers, Table 11. However, despite the low dosage of $CaCl_2$ showed an acceleration effect [123, 156], when a high dosage was used (e.g., 0.5 M), the setting time of the geopolymer matrix was retarded [156]. This retarding effect was not observed in

water-insoluble salts such as $Ca(OH)_2$, CaO, and $CaCO_3$ even for high dosage.

Besides the general heterogeneous nucleation, which has been suggested as the accelerating mechanism for the setting of geopolymers containing these additives, several secondary reactions occur. These are depending on the nature and concentration of the additives, geopolymer composition, and casting condition. For example, the acceleration effect of $CaCl_2$ addition has been described as the precipitation of alkali hydroxide, which can further react with the silicates to form C–S–H gel and promote the mechanical strength [156]. This mechanism is facilitated due to the high charge density and mobility of Cl^- which makes the gel porous, and therefore, provides a higher diffusion of water or alkaline solution. This results in a higher dissolution of aluminosilicates [123]. Another example is, a similar mechanical strength was expected when using the same molar content of $Ca(OH)_2$ and CaO as additives in the geopolymer, but the materials ended up with different strength. This has been correlated to incomplete hydrolysis of CaO in water due to the very short contact time of the experiment [156]. In the case of calcium aluminates, specifically dodecacalcium hepta-aluminate (C12A7), the acceleration in setting time has been attributed to the rapid formation of calcium aluminate or aluminosilicate hydrates as well as increasing the pH of the system to ease the dissolution of aluminosilicate precursors [135].

6.1.2.2. Mg-salts. Table 11 has shown a slight acceleration in setting time and an increase in early age strength when $MgCl_2$ and $Mg(NO_3)_2$ have been used as additives. This strength increase has been correlated with the production of intensive heterogeneous nucleation shortly upon the addition of the material [156].

6.2. Organic additives

Sucrose is a well-known organic retarder for OPC [157]. The retarding effect of sucrose additives has correlated to the conversion of HO–C–C═O groups from sucrose into acid complexes in an alkali environment. These acid complexes are supposed to be absorbed by the aluminosilicate particles, which hinders the nucleation of the dissolved products [123,155,158]. Furthermore, sucrose can be combined with ions available in geopolymer matrices such as Ca, Al, and Fe, and form insoluble metal-organic complexes, which covers the particles and delays the geopolymerization process. In contrast, carbohydrate-based compounds have been patented in any form of monomer (e.g., glucose), polymer (e.g., starch), or saccharide salt (e.g., carboxymethylcellulose) as setting accelerators in geopolymeric suspension [159]. However, this has been discussed to be dependent on the concentration of the additive used in the matrix. That means at high concentration sucrose can be an accelerator [123,154]. Furthermore, the addition of organic additives influences the final mechanical strength. According to Fig. 14, three effects can be seen; a) increase, b) no influence, and c) decrease in strength. Due to the limited data, these effects cannot be fully explained, and further work is required.

7. Conclusion and remarks

In several applications, understanding the setting time of geopolymers is as essential as the final mechanical strength. This review paper provides a holistic overview of factors that affect the hardening evolution of geopolymers as well as investigates the correlation between setting time of the fresh materials and final compressive strength. It was shown that the hardening of geopolymer is a function of several factors including the specific surface area, reactivity, chemical composition, and processing history of the materials. Different techniques were used to alter the aforementioned parameters, and consequently, control the hardening rate. Despite the ideal concept of changing the hardening of geopolymer at an early age while keeping the final strength unchanged, it is a nontrivial task to achieve it in most of the aluminosilicate precursors. This is mainly due to the complexity of the sources which contain a mixture of various particles, and each can have its own chemical composition, reactivity, and particle size. However, few examples showed that when the reactivity and particle size of the materials are known, by adjusting the chemical composition of the different geopolymers, the setting time of the material can be controllable while keeping the mechanical strength similar. An identical situation was also observed when the chemical composition of the material was kept constant while the crystalline structure of the aluminosilicate precursors was disordered. Based on the discussed facts, this study is a platform for further investigation on the feasibility of having geopolymers with controllable reactions independent on the utilized aluminosilicate precursors.

Declaration of competing interest

None.

Acknowledgment

This project has received funding from the European Union's Horizon 2020 research and innovation program under the Marie Sklodowska-Curie grant agreement no. 713683 (COFUNDfellowsDTU). M. Mehrali acknowledges support by a research grant (00025460) from VILLUM FONDEN. The authors would like to acknowledge the contribution of Dr. Toby Neville for fruitful discussions.

References

[1] M. Khalifeh, A. Saasen, T. Vralstad, H. Hodne, Potential utilization of class C fly ash-based geopolymer in oil well cementing operations, Cement Concr. Compos. 53 (2014) 10–17.
[2] O. Porcherie, E. Pershikova, Pumpable Geopolymer Formulation for Oilfield Application, Google Patents, 2011.
[3] J. Zhang, E.A. Weissinger, S. Peethamparan, G.W. Scherer, Early hydration and setting of oil well cement, Cement Concr. Res. 40 (7) (2010) 1023–1033.
[4] V.N. Nerella, S. Hempel, V. Mechtcherine, Effects of layer-interface properties on mechanical performance of concrete elements produced by extrusion-based 3D-printing, Construct. Build. Mater. 205 (2019) 586–601.
[5] G. Ma, Z. Li, L. Wang, Printable properties of cementitious material containing copper tailings for extrusion based 3D printing, Construct. Build. Mater. 162 (2018) 613–627.
[6] J.G. Sanjayan, B. Nematollahi, M. Xia, T. Marchment, Effect of surface moisture on inter-layer strength of 3D printed concrete, Construct. Build. Mater. 172 (2018) 468–475.
[7] D. Beaupre, Rheology of High Performance Shotcrete, University of British Columbia, 1994.
[8] S. Demie, M.F. Nuruddin, N. Shafiq, Effects of micro-structure characteristics of interfacial transition zone on the compressive strength of self-compacting geopolymer concrete, Construct. Build. Mater. 41 (2013) 91–98.
[9] B. Panda, S.C. Paul, L.J. Hui, Y.W.D. Tay, M.J. Tan, Additive manufacturing of geopolymer for sustainable built environment, J. Clean. Prod. 167 (2017) 281–288.
[10] B. Panda, M.J. Tan, Experimental study on mix proportion and fresh properties of fly ash based geopolymer for 3D concrete printing, Ceram. Int. 44 (9) (2018) 10258–10265.
[11] T. Glasby, J. Day, R. Genrich, J. Aldred, EFC geopolymer concrete aircraft pavements at Brisbane West Wellcamp Airport, Concrete 2015 (2015) 1–9.
[12] Z. Li, Y. Zhang, X. Zhou, Short fiber reinforced geopolymer composites manufactured by extrusion, J. Mater. Civ. Eng. 17 (6) (2005) 624–631.
[13] Z. Yunsheng, S. Wei, L. Zongjin, Impact behavior and microstructural characteristics of PVA fiber reinforced fly ash-geopolymer boards prepared by extrusion technique, J. Mater. Sci. 41 (10) (2006) 2787–2794.
[14] K. Okada, A. Imase, T. Isobe, A. Nakajima, Capillary rise properties of porous geopolymers prepared by an extrusion method using polylactic acid (PLA) fibers as the pore formers, J. Eur. Ceram. Soc. 31 (4) (2011) 461–467.
[15] L. Reiter, T. Wangler, N. Roussel, R.J. Flatt, The role of early age structural build-up in digital fabrication with concrete, Cement Concr. Res. 112 (2018) 86–95.
[16] R.A. Buswell, W.R. Leal de Silva, S.Z. Jones, J. Dirrenberger, 3D printing using concrete extrusion: a roadmap for research, Cement Concr. Res. 112 (2018) 37–49.
[17] B. Singh, G. Ishwarya, M. Gupta, S.K. Bhattacharyya, Geopolymer concrete: a review of some recent developments, Construct. Build. Mater. 85 (2015) 78–90.
[18] E. Worrell, L. Price, N. Martin, C. Hendriks, L.O. Meida, Carbon dioxide emissions from the global cement industry, Annu. Rev. Energy Environ. 26 (1) (2001) 303–329.

[19] N. Müller, J. Harnisch, A Blueprint for a Climate Friendly Cement Industry, A Report Prepared for the WWF-Lafarge Conservation Partnership, WWF International, 2008. Switzerland.
[20] E. Gartner, Industrially interesting approaches to "low-CO_2" cements, Cement Concr. Res. 34 (9) (2004) 1489–1498.
[21] B.L. Damineli, F.M. Kemeid, P.S. Aguiar, V.M. John, Measuring the eco-efficiency of cement use, Cement Concr. Compos. 32 (8) (2010) 555–562.
[22] P. Duxson, A. Fernández-Jiménez, J.L. Provis, G.C. Lukey, A. Palomo, J.S.J. van Deventer, Geopolymer technology: the current state of the art, J. Mater. Sci. 42 (9) (2007) 2917–2933.
[23] J. Davidovits, Geopolymer Chemistry and Applications, Geopolymer Institute2008.
[24] J.L. Provis, J.S.J. Van Deventer, Geopolymers: Structures, Processing, Properties and Industrial Applications, Elsevier2009.
[25] N. Ranjbar, M. Zhang, Fiber-reinforced geopolymer composites: a review, Cement Concr. Compos. 107 (2020), 103498.
[26] J. Davidovits, Years of Successes and Failures in Geopolymer Applications. Market Trends and Potential Breakthroughs, Geopolymer 2002 Conference, Geopolymer Institute Saint-Quentin, France, Melbourne, Australia, 2002, 29.
[27] J. Aldred, J. Day, Is Geopolymer Concrete a Suitable Alternative to Traditional Concrete, 37th Conference on Our World in Concrete & Structures, 2012, pp. 29–31. Singapore.
[28] N. Ranjbar, C. Kuenzel, Influence of preheating of fly ash precursors to produce geopolymers, J. Am. Ceram. Soc. 100 (7) (2017) 3165–3174.
[29] Z. Zuhua, Y. Xiao, Z. Huajun, C. Yue, Role of water in the synthesis of calcined kaolin-based geopolymer, Appl. Clay Sci. 43 (2) (2009) 218–223.
[30] H. Wang, H. Li, F. Yan, Synthesis and mechanical properties of metakaolinite-based geopolymer, Colloid. Surface. Physicochem. Eng. Aspect. 268 (1) (2005) 1–6.
[31] L. Weng, K. Sagoe-Crentsil, Dissolution processes, hydrolysis and condensation reactions during geopolymer synthesis: Part I—low Si/Al ratio systems, J. Mater. Sci. 42 (9) (2007) 2997–3006.
[32] A. Fernández-Jiménez, A. Palomo, M. Criado, Microstructure development of alkali-activated fly ash cement: a descriptive model, Cement Concr. Res. 35 (6) (2005) 1204–1209.
[33] J. Davidovits, Properties of Geopolymer Cements, First International Conference on Alkaline Cements and Concretes, Scientific Research Institute on Binders and Materials Kiev State Technical University, 1994, pp. 131–149. Ukraine.
[34] A. Hajimohammadi, J.L. Provis, J.S. Van Deventer, Effect of alumina release rate on the mechanism of geopolymer gel formation, Chem. Mater. 22 (18) (2010) 5199–5208.
[35] Sindhunata, J.S.J. van Deventer, G.C. Lukey, H. Xu, Effect of curing temperature and silicate concentration on fly-ash-based geopolymerization, Ind. Eng. Chem. Res. 45 (10) (2006) 3559–3568.
[36] G. Görhan, G. Kürklü, The influence of the NaOH solution on the properties of the fly ash-based geopolymer mortar cured at different temperatures, Compos. B Eng. 58 (2014) 371–377.
[37] E.N. Kani, A. Allahverdi, Effects of curing time and temperature on strength development of inorganic polymeric binder based on natural pozzolan, J. Mater. Sci. 44 (12) (2009) 3088–3097.
[38] C. Kuenzel, T.P. Neville, S. Donatello, L. Vandeperre, A.R. Boccaccini, C. R. Cheeseman, Influence of metakaolin characteristics on the mechanical properties of geopolymers, Appl. Clay Sci. 83–84 (2013) 308–314.
[39] N. Ranjbar, C. Kuenzel, Cenospheres: a review, Fuel 207 (2017) 1–12.
[40] J.N.Y. Djobo, H.K. Tchakouté, N. Ranjbar, A. Elimbi, L.N. Tchadjié, D. Njopwouo, Gel composition and strength properties of alkali-activated oyster shell-volcanic ash: effect of synthesis conditions, J. Am. Ceram. Soc. 99 (9) (2016) 3159–3166.
[41] J.L. Provis, S.A. Bernal, Geopolymers and related alkali-activated materials, Annu. Rev. Mater. Res. 44 (2014) 299–327.
[42] N. Ranjbar, A. Kashefi, M.R. Maheri, Hot-pressed geopolymer: dual effects of heat and curing time, Cement Concr. Compos. 86 (2018) 1–8.
[43] H. Sleiman, A. Perrot, S. Amziane, A new look at the measurement of cementitious paste setting by Vicat test, Cement Concr. Res. 40 (5) (2010) 681–686.
[44] S. Puligilla, P. Mondal, Role of slag in microstructural development and hardening of fly ash-slag geopolymer, Cement Concr. Res. 43 (2013) 70–80.
[45] D. Hardjito, M. Tsen, Strength and Thermal Stability of Fly Ash-Based Geopolymer Mortar, The 3rd International Conference-ACF/VCA, 2008, pp. 144–150.
[46] H. Wack, Zum Quellungsdruck von polymeren Hydrogelen, Fraunhofer-IRB-Verlag2007.
[47] L. Nachbaur, J.C. Mutin, A. Nonat, L. Choplin, Dynamic mode rheology of cement and tricalcium silicate pastes from mixing to setting, Cement Concr. Res. 31 (2) (2001) 183–192.
[48] A. Papo, B. Caufin, A study of the hydration process of cement pastes by means of oscillatory rheological techniques, Cement Concr. Res. 21 (6) (1991) 1111–1117.
[49] P.F.G. Banfill, R.E. Carter, P.J. Weaver, Simultaneous rheological and kinetic measurements on cement pastes, Cement Concr. Res. 21 (6) (1991) 1148–1154.
[50] A. Favier, Mécanisme de prise et rhéologie de liants géopolymères modèles, Paris Est, 2013.
[51] S. Wallah, B.V. Rangan, Low-calcium Fly Ash-Based Geopolymer Concrete: Long-Term Properties, 2006.
[52] D. Hardjito, S.E. Wallah, D.M. Sumajouw, B.V. Rangan, On the development of fly ash-based geopolymer concrete, Mater. J. 101 (6) (2004) 467–472.
[53] I.A. Rahman, P. Vejayakumaran, C.S. Sipaut, J. Ismail, C.K. Chee, Size-dependent physicochemical and optical properties of silica nanoparticles, Mater. Chem. Phys. 114 (1) (2009) 328–332.
[54] M. De Souza, W. Magalhães, M. Persegil, Silica derived from burned rice hulls, Mater. Res. 5 (4) (2002) 467–474.
[55] S. Kumar, R. Kumar, Mechanical activation of fly ash: effect on reaction, structure and properties of resulting geopolymer, Ceram. Int. 37 (2) (2011) 533–541.
[56] P. Chindaprasirt, T. Chareerat, S. Hatanaka, T. Cao, High-strength geopolymer using fine high-calcium fly ash, J. Mater. Civ. Eng. 23 (3) (2010) 264–270.
[57] G. du Toit, E.M. van der Merwe, E.P. Kearsley, M. McDonald, R.A. Kruger, Compressive Strength of Chemically and Mechanically Activated Aluminosilicate Systems, 2015 World of Coal Ash Conference in Nasvhille, 2015.
[58] N. Marjanović, M. Komljenović, Z. Baščarević, V. Nikolić, Improving reactivity of fly ash and properties of ensuing geopolymers through mechanical activation, Construct. Build. Mater. 57 (2014) 151–162.
[59] J.N. Yankwa Djobo, A. Elimbi, H.K. Tchakoute, S. Kumar, Mechanical activation of volcanic ash for geopolymer synthesis: effect on reaction kinetics, gel characteristics, physical and mechanical properties, RSC Adv. 6 (45) (2016) 39106–39117.
[60] C. Heah, K. Hussin, M.M. Al Bakri Abdullah, M. Bnhussain, L. Musa, I. Khairul Nizar, C.M.R. Ghazali, Y. Liew, Strength and Microstructural Properties of Mechanically-Activated Kaolin Geopolymers, Advanced Materials Research, Trans Tech Publ, 2013, pp. 926–930.
[61] L. Weng, K. Sagoe-Crentsil, T. Brown, S. Song, Effects of aluminates on the formation of geopolymers, Mater. Sci. Eng., B 117 (2) (2005) 163–168.
[62] J. Temuujin, R. Williams, A. Van Riessen, Effect of mechanical activation of fly ash on the properties of geopolymer cured at ambient temperature, J. Mater. Process. Technol. 209 (12–13) (2009) 5276–5280.
[63] C. Lanzerstorfer, Fly ash from coal combustion: dependence of the concentration of various elements on the particle size, Fuel 228 (2018) 263–271.
[64] G. Mucsi, S. Kumar, B. Csőke, R. Kumar, Z. Molnár, Á. Rácz, F. Mádai, Á. Debreczeni, Control of geopolymer properties by grinding of land filled fly ash, Int. J. Miner. Process. 143 (2015) 50–58.
[65] J.N.Y. Djobo, A. Elimbi, H.K. Tchakouté, S. Kumar, Mechanical activation of volcanic ash for geopolymer synthesis: effect on reaction kinetics, gel characteristics, physical and mechanical properties, RSC Adv. 6 (45) (2016) 39106–39117.
[66] C. Kuenzel, N. Ranjbar, Dissolution mechanism of fly ash to quantify the reactive aluminosilicates in geopolymerisation, Resour. Conserv. Recycl. 150 (2019), 104421.
[67] R. Kumar, S. Kumar, S. Mehrotra, Towards sustainable solutions for fly ash through mechanical activation, Resour. Conserv. Recycl. 52 (2) (2007) 157–179.
[68] N. Ranjbar, M. Mehrali, M.R. Maheri, M. Mehrali, Hot-pressed geopolymer, Cement Concr. Res. 100 (2017) 14–22.
[69] E. Diaz, E. Allouche, S. Eklund, Factors affecting the suitability of fly ash as source material for geopolymers, Fuel 89 (5) (2010) 992–996.
[70] A. Elimbi, H.K. Tchakoute, D. Njopwouo, Effects of calcination temperature of kaolinite clays on the properties of geopolymer cements, Construct. Build. Mater. 25 (6) (2011) 2805–2812.
[71] Y. Hu, S. Liang, J. Yang, Y. Chen, N. Ye, Y. Ke, S. Tao, K. Xiao, J. Hu, H. Hou, W. Fan, S. Zhu, Y. Zhang, B. Xiao, Role of Fe species in geopolymer synthesized from alkali-thermal pretreated Fe-rich Bayer red mud, Construct. Build. Mater. 200 (2019) 398–407.
[72] T. Feng, R. Pinal, M.T. Carvajal, Process induced disorder in crystalline materials: differentiating defective crystals from the amorphous form of griseofulvin, J. Pharmaceut. Sci. 97 (8) (2008) 3207–3221.
[73] H. Li, D. Xu, S. Feng, B. Shang, Microstructure and performance of fly ash micro-beads in cementitious material system, Construct. Build. Mater. 52 (2014) 422–427.
[74] J.-B. Zhang, S.-P. Li, H.-Q. Li, M.-M. He, Acid activation for pre-desilicated high-alumina fly ash, Fuel Process. Technol. 151 (2016) 64–71.
[75] A.M. Kalinkin, S. Kumar, B.I. Gurevich, T.C. Alex, E.V. Kalinkina, V. V. Tyukavkina, V.T. Kalinnikov, R. Kumar, Geopolymerization behavior of Cu–Ni slag mechanically activated in air and in CO_2 atmosphere, Int. J. Miner. Process. 112–113 (2012) 101–106.
[76] V. Saraswathy, S. Muralidharan, K. Thangavel, S. Srinivasan, Influence of activated fly ash on corrosion-resistance and strength of concrete, Cement Concr. Compos. 25 (7) (2003) 673–680.
[77] J. Rocha, J.M. Adams, J. Klinowski, The rehydration of metakaolinite to kaolinite: evidence from solid-state NMR and cognate techniques, J. Solid State Chem. 89 (2) (1990) 260–274.
[78] J. Sanz, A. Madani, J.M. Serratosa, J.S. Moya, S. Aza, Aluminum-27 and silicon-29 magic-angle spinning nuclear magnetic resonance study of the kaolinite-mullite transformation 71 (10) (1988) C418–C421.
[79] C. Künzel, Metakaolin Based Geopolymers to Encapsulate Nuclear Waste, Imperial College London, 2013.
[80] S. Lee, Y.J. Kim, H.-S. Moon, Energy-filtering transmission electron microscopy (EF-TEM) study of a modulated structure in metakaolinite, Modulation 86 (1) (2003) 174–176. Represented by a 14 Å.
[81] B.B. Kenne Diffo, A. Elimbi, M. Cyr, J. Dika Manga, H. Tchakoute Kouamo, Effect of the rate of calcination of kaolin on the properties of metakaolin-based geopolymers, J. Asian Ceram. Soc. 3 (1) (2015) 130–138.
[82] R.C. Kaze, L.M. Beleuk à Moungam, M.L. Fonkwe Djouka, A. Nana, E. Kamseu, U. F. Chinje Melo, C. Leonelli, The corrosion of kaolinite by iron minerals and the effects on geopolymerization, Appl. Clay Sci. 138 (2017) 48–62.

[83] A. Sharma, K. Srivastava, V. Devra, A.J. Rani, Modification in properties of fly ash through mechanical and chemical activation, Am. Chem. Sci. J. vol. 2 (4) (2012) 177–187.

[84] A. G Patil, S. Anandhan, Ball milling of class-F Indian fly ash obtained from a thermal power station, International Journal of Energy Engineering 2 (2) (2012) 57–62.

[85] A.D. Hounsi, G.L. Lecomte-Nana, G. Djétéli, P. Blanchart, Kaolin-based geopolymers: effect of mechanical activation and curing process, Construct. Build. Mater. 42 (2013) 105–113.

[86] L. Kriskova, Y. Pontikes, Ö. Cizer, G. Mertens, W. Veulemans, D. Geysen, P. T. Jones, L. Vandewalle, K. Van Balen, B. Blanpain, Effect of mechanical activation on the hydraulic properties of stainless steel slags, Cement Concr. Res. 42 (6) (2012) 778–788.

[87] K.L. Aughenbaugh, Fly Ash-Based Geopolymers: Identifying Reactive Glassy Phases in Potential Raw Materials, 2013.

[88] S. Ohsawa, K. Asaga, S. Goto, M. Daimon, Quantitative determination of fly ash in the hydrated fly ash-$CaSO_4{\cdot}2H_2O.Ca(OH)_2$ system, Cement Concr. Res. 15 (2) (1985) 357–366.

[89] J.L. Provis, J.S. van Deventer, Geopolymerisation kinetics. 1. In situ energy-dispersive X-ray diffractometry, Chem. Eng. Sci. 62 (9) (2007) 2309–2317.

[90] J. Provis, J. Van Deventer, Geopolymerisation kinetics. 2. Reaction kinetic modelling, Chem. Eng. Sci. 62 (9) (2007) 2318–2329.

[91] K. Sagoe-Crentsil, L. Weng, Dissolution processes, hydrolysis and condensation reactions during geopolymer synthesis: Part II. High Si/Al ratio systems, J. Mater. Sci. 42 (9) (2007) 3007–3014.

[92] A. Fernández-Jiménez, A. Palomo, I. Sobrados, J. Sanz, The role played by the reactive alumina content in the alkaline activation of fly ashes, Microporous Mesoporous Mater. 91 (1) (2006) 111–119.

[93] C. Catlow, A. George, C. Freeman, Ab initio and molecular-mechanics studies of aluminosilicate fragments, and the origin of Lowenstein's rule, Chem. Commun. (11) (1996) 1311–1312.

[94] Z.-h. Zhang, X. Yao, H.-j. Zhu, S.-d. Hua, Y. Chen, Preparation and mechanical properties of polypropylene fiber reinforced calcined kaolin-fly ash based geopolymer, J. Cent. S. Univ. Technol. 16 (1) (2009) 49–52.

[95] Z. Zhang, H. Wang, Y. Zhu, A. Reid, J.L. Provis, F. Bullen, Using fly ash to partially substitute metakaolin in geopolymer synthesis, Appl. Clay Sci. 88–89 (2014) 194–201.

[96] X. Gao, Q.L. Yu, H.J.H. Brouwers, Characterization of alkali activated slag–fly ash blends containing nano-silica, Construct. Build. Mater. 98 (2015) 397–406.

[97] E. Nimwinya, W. Arjharn, S. Horpibulsuk, T. Phoo-ngernkham, A. Poowancum, A sustainable calcined water treatment sludge and rice husk ash geopolymer, J. Clean. Prod. 119 (2016) 128–134.

[98] P. Duxson, S.W. Mallicoat, G.C. Lukey, W.M. Kriven, J.S. van Deventer, The effect of alkali and Si/Al ratio on the development of mechanical properties of metakaolin-based geopolymers, Colloid. Surface. Physicochem. Eng. Aspect. 292 (1) (2007) 8–20.

[99] H.W. Nugteren, M.B. Ogundiran, G.-J. Witkamp, M. Kreutzer, Coal Fly Ash Activated by Waste Sodium Aluminate Solutions as an Immobilizer for Hazardous Waste, Proceedings of the 2011 World Coal Ash WOCA Conference, Denver, CO, USA, 2011, pp. 9–11.

[100] N.K. Lee, H.K. Lee, Setting and mechanical properties of alkali-activated fly ash/slag concrete manufactured at room temperature, Construct. Build. Mater. 47 (2013) 1201–1209.

[101] P. Risdanareni, J.J. Ekaputri, M.M. Al Bakri Abdullah, Effect of Alkaline Activator Ratio to Mechanical Properties of Geopolymer Concrete with Trass as Filler, Applied Mechanics and Materials, Trans Tech Publ, 2015, pp. 406–412.

[102] P. Nath, P.K. Sarker, Use of OPC to improve setting and early strength properties of low calcium fly ash geopolymer concrete cured at room temperature, Cement Concr. Compos. 55 (2015) 205–214.

[103] S.W. Wijaya, D. Hardjito, Factors Affecting the Setting Time of Fly Ash-Based Geopolymer, Materials Science Forum, Trans Tech Publ, 2016, pp. 90–97.

[104] T. Bakharev, J.G. Sanjayan, Y.-B. Cheng, Alkali activation of Australian slag cements, Cement Concr. Res. 29 (1) (1999) 113–120.

[105] S.A. Bernal, J.L. Provis, V. Rose, R. Mejía de Gutierrez, Evolution of binder structure in sodium silicate-activated slag-metakaolin blends, Cement Concr. Compos. 33 (1) (2011) 46–54.

[106] A. Fernández-Jiménez, F. Puertas, Setting of alkali-activated slag cement. Influence of activator nature, Adv. Cement Res. 13 (3) (2001) 115–121.

[107] P.D. Silva, K. Sagoe-Crenstil, V. Sirivivatnanon, Kinetics of geopolymerization: role of Al2O3 and SiO2, Cement Concr. Res. 37 (4) (2007) 512–518.

[108] K. Gao, K.-L. Lin, D. Wang, C.-L. Hwang, H.-S. Shiu, Y.-M. Chang, T.-W. Cheng, Effects SiO_2/Na_2O molar ratio on mechanical properties and the microstructure of nano-SiO_2 metakaolin-based geopolymers, Construct. Build. Mater. 53 (2014) 503–510.

[109] T. Rahmiati, K.A. Azizli, Z. Man, L. Ismail, M.F. Nuruddin, The Effect of KOH Concentration on Setting Time and Compressive Strength of Fly Ash-Based Geopolymer, Applied Mechanics and Materials, Trans Tech Publ, 2014, pp. 94–97.

[110] A. Poulesquen, F. Frizon, D. Lambertin, Rheological behavior of alkali-activated metakaolin during geopolymerization, J. Non-Cryst. Solids 357 (21) (2011) 3565–3571.

[111] H. Xu, J. Van Deventer, The geopolymerisation of alumino-silicate minerals, Int. J. Miner. Process. 59 (3) (2000) 247–266.

[112] D.L. Kong, J.G. Sanjayan, K. Sagoe-Crentsil, Factors affecting the performance of metakaolin geopolymers exposed to elevated temperatures, J. Mater. Sci. 43 (3) (2008) 824–831.

[113] M. Lizcano, H.S. Kim, S. Basu, M. Radovic, Mechanical properties of sodium and potassium activated metakaolin-based geopolymers, J. Mater. Sci. 47 (6) (2012) 2607–2616.

[114] J. Davidovits, Geopolymers: inorganic polymeric new materials, J. Therm. Anal. Calorim. 37 (8) (1991) 1633–1656.

[115] R. Robayo, R.M. De Gutiérrez, M. Gordillo, Natural pozzolan-and granulated blast furnace slag-based binary geopolymers, Mater. Construcción 66 (321) (2016), 077.

[116] M. Vafaei, A. Allahverdi, Influence of calcium aluminate cement on geopolymerization of natural pozzolan, Construct. Build. Mater. 114 (2016) 290–296.

[117] S. Kumar, R. Kumar, S.P. Mehrotra, Influence of granulated blast furnace slag on the reaction, structure and properties of fly ash based geopolymer, J. Mater. Sci. 45 (3) (2010) 607–615.

[118] I. García-Lodeiro, A. Palomo, A. Fernández-Jiménez, D.J.C. Macphee, C. Research, Compatibility studies between NASH and CASH gels. Study in the ternary diagram Na_2O–CaO–Al_2O_3–SiO_2–H_2O 41 (9) (2011) 923–931.

[119] C.K. Yip, G.C. Lukey, J.L. Provis, J.S.J. van Deventer, Effect of calcium silicate sources on geopolymerisation, Cement Concr. Res. 38 (4) (2008) 554–564.

[120] S. Alonso, A.J.C. Palomo, C. Research, Calorimetric Study of Alkaline Activation of Calcium Hydroxide–Metakaolin Solid Mixtures vol. 31, 2001, pp. 25–30, 1.

[121] C.K. Yip, G. Lukey, J. Van Deventer, The coexistence of geopolymeric gel and calcium silicate hydrate at the early stage of alkaline activation, Cement Concr. Res. 35 (9) (2005) 1688–1697.

[122] M.L. Granizo, S. Alonso, M.T. Blanco-Varela, A. Palomo, Alkaline activation of metakaolin: effect of calcium hydroxide in the products of reaction, J. Am. Ceram. Soc. 85 (1) (2002) 225–231.

[123] U. Rattanasak, K. Pankhet, P. Chindaprasirt, Effect of chemical admixtures on properties of high-calcium fly ash geopolymer, Int. J. Miner. Metal. Mater. 18 (3) (2011) 364.

[124] S. Chithiraputhiran, N. Neithalath, Isothermal reaction kinetics and temperature dependence of alkali activation of slag, fly ash and their blends, Construct. Build. Mater. 45 (2013) 233–242.

[125] Y. Djobo, A. Elimbi, J.D. Manga, I.D.L. Ndjock, Partial replacement of volcanic ash by bauxite and calcined oyster shell in the synthesis of volcanic ash-based geopolymers, Construct. Build. Mater. 113 (2016) 673–681.

[126] A. Buchwald, K. Dombrowski, M. Weil, The influence of calcium content on the performance of geopolymeric binder especially the resistance against acids, Proc. World Geopolym. (2005) 35–39.

[127] S. Pangdaeng, T. Phoo-ngernkham, V. Sata, P. Chindaprasirt, Influence of curing conditions on properties of high calcium fly ash geopolymer containing Portland cement as additive, Mater. Des. 53 (2014) 269–274.

[128] C. Li, H. Sun, L. Li, A review: the comparison between alkali-activated slag (Si+Ca) and metakaolin (Si+Al) cements, Cement Concr. Res. 40 (9) (2010) 1341–1349.

[129] S. Saha, C. Rajasekaran, Enhancement of the properties of fly ash based geopolymer paste by incorporating ground granulated blast furnace slag, Construct. Build. Mater. 146 (2017) 615–620.

[130] M.N.S. Hadi, N.A. Farhan, M.N. Sheikh, Design of geopolymer concrete with GGBFS at ambient curing condition using Taguchi method, Construct. Build. Mater. 140 (2017) 424–431.

[131] G. Mallikarjuna Rao, T.D. Gunneswara Rao, Final setting time and compressive strength of fly ash and GGBS-based geopolymer paste and mortar, Arabian J. Sci. Eng. 40 (11) (2015) 3067–3074.

[132] I. Perná, T. Hanzlíček, The setting time of a clay-slag geopolymer matrix: the influence of blast-furnace-slag addition and the mixing method, J. Clean. Prod. 112 (2016) 1150–1155.

[133] T. Phoo-ngernkham, P. Chindaprasirt, V. Sata, S. Pangdaeng, T. Sinsiri, Properties of high calcium fly ash geopolymer pastes with Portland cement as an additive, Int. J. Miner., Metal. Mater. 20 (2) (2013) 214–220.

[134] T. Suwan, M. Fan, Influence of OPC replacement and manufacturing procedures on the properties of self-cured geopolymer, Construct. Build. Mater. 73 (2014) 551–561.

[135] P. Rovnanik, Influence of C12A7 admixture on setting properties of fly ash geopolymer, Ceramics 54 (4) (2010) 362–367.

[136] Y. Liew, H. Kamarudin, A. Al Bakri, M. Binhussain, L. Musa, I. Khairul Nizar, C.M. R. Ghazali, C. Heah, Calcined Kaolin Geopolymeric Powder: Influence of Water-To-Geopolymeric Powder Ratio, Advanced Materials Research, Trans Tech Publ, 2012, pp. 48–53.

[137] B.V. Rangan, Fly Ash-Based Geopolymer Concrete, 2008.

[138] S. Yaseri, G. Hajiaghaei, F. Mohammadi, M. Mahdikhani, R. Farokhzad, The role of synthesis parameters on the workability, setting and strength properties of binary binder based geopolymer paste, Construct. Build. Mater. 157 (2017) 534–545.

[139] H.E. Elyamany, A.E.M. Abd Elmoaty, A.M. Elshaboury, Setting time and 7-day strength of geopolymer mortar with various binders, Construct. Build. Mater. 187 (2018) 974–983.

[140] S. Park, M. Pour-Ghaz, What is the role of water in the geopolymerization of metakaolin? Construct. Build. Mater. 182 (2018) 360–370.

[141] D.P. Bentz, M.A. Peltz, J. Winpigler, Early-age properties of cement-based materials. II: influence of water-to-cement ratio, J. Mater. Civ. Eng. 21 (9) (2009) 512–517.

[142] S. Amziane, Setting time determination of cementitious materials based on measurements of the hydraulic pressure variations, Cement Concr. Res. 36 (2) (2006) 295–304.

[143] S.A. Bernal, J.L. Provis, A. Fernández-Jiménez, P.V. Krivenko, E. Kavalerova, M. Palacios, C. Shi, Binder Chemistry–High-Calcium Alkali-Activated Materials, Alkali activated materials, Springer2014, pp. 59-91.
[144] A.A. Aliabdo, A.E.M. Abd Elmoaty, H.A. Salem, Effect of water addition, plasticizer and alkaline solution constitution on fly ash based geopolymer concrete performance, Construct. Build. Mater. 121 (2016) 694–703.
[145] C. Kuenzel, Geopolymers for Nuclear Waste Encapsulation, Imperial College London, 2010.
[146] B.-h. Mo, H. Zhu, X.-m. Cui, Y. He, S.-y. Gong, Effect of curing temperature on geopolymerization of metakaolin-based geopolymers, Appl. Clay Sci. 99 (2014) 144–148.
[147] T.W. Cheng, J.P. Chiu, Fire-resistant geopolymer produced by granulated blast furnace slag, Miner. Eng. 16 (3) (2003) 205–210.
[148] J. Wang, T. Cheng, Production Geopolymer Materials by Coal Fly Ash, Proceedings of the 7th International Symposium on East Asian Resources Recycling Technology, 2003, 266.
[149] P. Rovnaník, Effect of curing temperature on the development of hard structure of metakaolin-based geopolymer, Construct. Build. Mater. 24 (7) (2010) 1176–1183.
[150] P. Nath, P.K. Sarker, Effect of GGBFS on setting, workability and early strength properties of fly ash geopolymer concrete cured in ambient condition, Construct. Build. Mater. 66 (2014) 163–171.
[151] O. Burciaga-Díaz, L.Y. Gómez-Zamorano, J.I. Escalante-García, Influence of the long term curing temperature on the hydration of alkaline binders of blast furnace slag-metakaolin, Construct. Build. Mater. 113 (2016) 917–926.
[152] H.-G. Park, S.-K. Sung, C.-G. Park, J.-P. Won, Influence of a C12A7 mineral-based accelerator on the strength and durability of shotcrete, Cement Concr. Res. 38 (3) (2008) 379–385.
[153] J. Ding, Y. Fu, J.J. Beaudoin, Study of hydration mechanisms in the high alumina cement - sodium silicate system, Cement Concr. Res. 26 (5) (1996) 799–804.
[154] N.B. Singh, A.K. Singh, S. Prabha Singh, Effect of citric acid on the hydration of portland cement, Cement Concr. Res. 16 (6) (1986) 911–920.
[155] A. Kusbiantoro, M.S. Ibrahim, K. Muthusamy, A. Alias, Development of sucrose and citric acid as the natural based admixture for fly ash based geopolymer, Procedia Environ. Sci. 17 (2013) 596–602.
[156] W.K.W. Lee, J.S.J. van Deventer, The effect of ionic contaminants on the early-age properties of alkali-activated fly ash-based cements, Cement Concr. Res. 32 (4) (2002) 577–584.
[157] G. Bruere, Set-retarding effects of sugars in Portland cement pastes, Nature 212 (5061) (1966), 502.
[158] F. Nuruddin, A. Kusbiantoro, S. Qazi, N. Shafiq, The Effect of Natural Retarder on Fly Ash Based Geopolymer Concrete, 2010.
[159] E. Pershikova, O. Porcherie, S. Kefi, Y. Boubeguira, H. Achtal, Pumpable Geopolymers Comprising a Setting Accelerator, Google Patents, 2015.